NASA MEMO 5-25-59L

NASA

MEMORANDUM

INVESTIGATION OF THE STABILITY OF VERY FLAT SPINS AND ANALYSIS OF EFFECTS OF APPLYING VARIOUS MOMENTS UTILIZING THE THREE MOMENT EQUATIONS OF MOTION

By Walter J. Klinar and William D. Grantham

Langley Research Center
Langley Field, Va.

NATIONAL AERONAUTICS AND SPACE ADMINISTRATION
WASHINGTON
June 1959

NATIONAL AERONAUTICS AND SPACE ADMINISTRATION

MEMORANDUM 5-25-59L

INVESTIGATION OF THE STABILITY OF VERY FLAT SPINS AND ANALYSIS OF EFFECTS OF APPLYING VARIOUS MOMENTS UTILIZING THE THREE MOMENT EQUATIONS OF MOTION

By Walter J. Klinar and William D. Grantham

SUMMARY

Based on linearized equations of motion utilizing only the three moment equations and assuming only flat-spin conditions, it appears that contemporary designs (with the moment of inertia about the wing axis I_Y considerably greater than the moment of inertia about the fuselage axis I_X) having positive values of C_{l_p} (rolling-moment coefficient due to rolling) or positive values of C_{l_β} (rolling-moment coefficient due to sideslip) will probably not have a stable spin in the flat-spin region near an angle of attack of 90°. If the damping in pitch in flat-spin attitudes is zero, stable flat-spin conditions may not be possible on an airplane having the mass primarily distributed along the wings. The effect of moving ailerons with the spin or the effect of applying a positive pitching moment producing recovery for contemporary fighter designs will be greatest for large negative values of C_{n_β} (yawing-moment coefficient due to sideslip). In addition, for a certain critical value of positive C_{n_β}, the rolling moment applied by moving ailerons with the spin or the application of a positive pitching moment will have no effect on reducing the spin rate.

INTRODUCTION

Flat spins of airplanes have become more prevalent than in the past, along with the trends toward lengthened fuselage forebodies, increased relative distribution of mass in the fuselage, and low-span wings. Research results, in general, have indicated the important effects of such factors as mass distribution and fuselage-nose cross-sectional shape on the overall stability of a potential spinning motion in determining the nature of spins achieved for current configurations.

As regards the effect of fuselage-nose cross-sectional shape, results of investigations of dynamic models in the Langley 20-foot free-spinning tunnel and of static tests in the Langley 300-MPH 7- by 10-foot tunnel (refs. 1 and 2) have indicated that certain fuselage cross-sectional shapes can provide propelling moments at flat-spin attitudes which might make an airplane have an uncontrollable flat spin with a high rotational rate. Spin-model tests have also shown, however, that, for certain models of contemporary fighters which had propelling noses, the flat spin was not a stable condition but that the motion of the model appeared to be oscillatorily divergent in roll. This oscillatory roll divergence, when it occurs, generally causes the spin rate of the model to decrease and the model either ceases to spin or assumes a steeper spin attitude with a slower rotational rate. The mass distribution of models for which this motion has been observed is such that most of the mass is extended along the fuselage (the moment of inertia about the wing axis I_Y is high) and the wings are relatively light (the moment of inertia about the fuselage axis I_X is low). From the results of the aforementioned spin-model tests, it is considered desirable that a given airplane be unstable in the flat-spin region and that the aerodynamic or mass characteristics should be arranged so that there is no possibility of a stable flat spin.

Accordingly, an analytical investigation was undertaken to determine how a flat-spin condition, on a specific design, would be influenced by stability characteristics. This problem is analyzed herein by utilizing only the linearized pitch, roll, and yaw equations of motion. This approach seems reasonable inasmuch as model force-test data show little change in the aerodynamic forces for small sideslip angles and for variations in angle of attack in the flat-spin region. Also, as stated in reference 3, the recovery motion of the airplane appears to be affected primarily by the action of the moments rather than of the forces. The effects of applying various moments in a flat spin have been examined.

SYMBOLS

The body system of axes is used. This system of axes, related angles, and positive directions of corresponding forces and moments are illustrated in figure 1. The symbols are defined as follows:

C_l rolling-moment coefficient, $\dfrac{M_X}{\frac{1}{2}\rho V^2 Sb}$

C_m pitching-moment coefficient, $\frac{M_Y}{\frac{1}{2}\rho V^2 Sb}$

C_n yawing-moment coefficient, $\frac{M_Z}{\frac{1}{2}\rho V^2 Sb}$

$C_1, C_2, C_3, C_4, C_5, C_6$ coefficients of characteristic equation (eq. (A19))

M_X rolling moment acting about X body axis, ft-lb

M_Y pitching moment acting about Y body axis, ft-lb

M_Z yawing moment acting about Z body axis, ft-lb

Δ difference between two values

t time, sec

S wing area, sq ft

b wing span, ft

ρ air density, slugs/cu ft

V resultant linear velocity, ft/sec

Ω resultant angular velocity, radians/sec

λ roots of characteristic equation

$M_{Y_\theta} = \frac{\partial M_Y}{\partial \theta}$ ft-lb/radian

$M_{Z_\beta} = \frac{\partial M_Z}{\partial \beta}$ ft-lb/radian

$M_{X_\beta} = \frac{\partial M_X}{\partial \beta}$ ft-lb/radian

$M_{X_p} = \frac{\partial M_X}{\partial p}$ ft-lb-sec/radian

$M_{X_r} = \frac{\partial M_X}{\partial r}$ ft-lb-sec/radian

$M_{Y_q} = \frac{\partial M_Y}{\partial q}$ ft-lb-sec/radian

$M_{Z_r} = \frac{\partial M_Z}{\partial r}$ ft-lb-sec/radian

$M_{Z_p} = \frac{\partial M_Z}{\partial p}$ ft-lb-sec/radian

X,Y,Z longitudinal, lateral, and vertical body axes, respectively

p,q,r components of angular velocity about X, Y, and Z body axes, respectively, radians/sec

r_o value of r before disturbance, radians/sec

I_X,I_Y,I_Z moments of inertia about X, Y, and Z body axes, respectively, slug-ft^2

θ angular displacement of X body axis from horizontal plane measured in vertical plane, positive when airplane nose is above horizontal plane, deg or radians

ϕ total angular movement of Y body axis from horizontal plane measured in YZ body plane, positive when clockwise as viewed from rear of airplane (if X body axis is vertical, ϕ is measured from a reference position in horizontal plane), deg or radians

α angle of attack, angle between relative wind V projected into XZ-plane of symmetry and X body axis, positive when relative wind comes from below XY body plane, deg or radians

β angle of sideslip, angle between relative wind V and projection of relative wind on XZ-plane, positive when relative wind comes from right of plane of symmetry, deg or radians

ψ horizontal component of total angular deflection of X body axis from reference position in horizontal plane, positive when clockwise as viewed from vertically above airplane, radians

$F(d)$ characteristic (or stability) equation

$f(d)$ numerator of equation for motion after various forcing functions are applied

$$C_{l_p} = \frac{\partial C_l}{\partial \frac{pb}{2V}}$$

$$C_{n_r} = \frac{\partial C_n}{\partial \frac{rb}{2V}}$$

$$C_{m_q} = \frac{\partial C_m}{\partial \frac{qb}{2V}}$$

$$C_{l_\beta} = \frac{\partial C_l}{\partial \beta} \text{ per radian}$$

$$C_{m_\theta} = \frac{\partial C_m}{\partial \theta} \text{ per radian}$$

$$C_{n_\beta} = \frac{\partial C_n}{\partial \beta} \text{ per radian}$$

$K_{\Delta\theta}$ constant value in $\Delta\theta$ forcing-function equation (eq. (5))

$K_{\Delta r}$ constant value in Δr forcing-function equation (eq. (4))

$$D = \frac{d}{dt}$$

Subscripts and superscripts:

o initial

t time

A dot over a symbol represents the derivative with respect to time; for example, $\dot{\phi} = \frac{d\phi}{dt}$.

METHODS AND APPROXIMATIONS

Three degrees of freedom were utilized in the present investigation. The moment equations of motion were used to correspond with these degrees of freedom and are presented in appendix A as equations (A1) to (A3). As indicated in these equations, the body axes and principal axes are assumed to coincide, and the engine gyroscopic moments are neglected. Also, it was assumed that the airplane was spinning about its center of gravity in a completely steady spin; that is, $\dot{p}$, $\dot{q}$, and $\dot{r}$ were zero. For these steady spins, the sideslip angle was assumed to be zero and in order to achieve equilibrium at zero sideslip a small amount of rolling moment ΔM_X was applied to oppose the rolling moment generated by $M_{X_p}p$ and a small amount of yawing moment ΔM_Z to oppose $M_{Z_r}r$.

The slope of the pitching-moment curve M_{Y_θ} is the same as the pitching moment plotted against angle of attack. The plot of pitching moment against θ would have the form similar to that indicated in figure 2. In addition, the pitching-moment coefficients were nondimensionalized with respect to the wing span b instead of the chord.

The aerodynamic derivatives used were assumed to be constant for the flat-spin attitudes assumed, and such derivatives as M_{X_r} and M_{Z_p} were considered to be small enough to be neglected.

Because of the fundamental assumptions made for the flat-spin condition assumed, which would be near an angle of attack of 90°, the following conditions existed:

(a) The rate of descent V remained constant and was the resultant velocity (determined by equating the drag at the spin angle of attack to the weight of the airplane).

(b) The rate of yawing r was equal to the resultant rotational rate about the spin axis Ω or $\dot{\psi}$.

(c) The sideslip angle β was the same as the wing-tilt angle about the body axis ϕ.

(d) The angle of attack α was equivalent to $90^\circ + \theta$, with θ being the inclination of the longitudinal axis of the airplane above the horizon. (Thus, for very flat spins, θ becomes a small negative angle.)

With these conditions, and from expressions of Euler's attitude angles in terms of the angular velocities about the body axes (appendix A), expressions for p, q, and r in terms of $\Delta\beta$, $\Delta\theta$, and Δr were obtained, with second-order terms being considered small enough to be neglected, and are presented as equations (A4) to (A6). From these equations, the equations of motion (eqs. (A1) to (A3)) about the three body axes are rewritten as equations (A16) to (A18). This procedure is used in order that only three variables describing the motion remain in the equations of motion, whereas originally there were five.

When equations (A16) to (A18) are placed in determinant form, the characteristic equation (eq. (A19)) can be determined and is of the form

$$C_1D^5 + C_2D^4 + C_3D^3 + C_4D^2 + C_5D + C_6 = 0.$$

The expression for the various coefficients of the quintic are contained in appendix A. The conditions necessary for the roots of equation (A19) to be stable (according to ref. 4) are that the coefficients of the equation all be positive and that certain functions of the coefficients known as Routh's discriminant also be positive. Routh's discriminant for the quintic equation is as follows:

$$C_2C_3 - C_1C_4 \tag{1}$$

$$C_4\left(C_2C_3 - C_1C_4\right) - C_2\left(C_2C_5 - C_1C_6\right) \tag{2}$$

$$\left(C_2C_5 - C_1C_6\right)\left[C_4\left(C_2C_3 - C_1C_4\right) - C_2\left(C_2C_5 - C_1C_6\right)\right] - C_6\left(C_2C_3 - C_1C_4\right)^2 \tag{3}$$

An alternate form of Routh's discriminant is given in reference 5. In order to investigate some of the factors that might affect the stability of the flat spin, the stability derivatives were varied in the stability equations for an airplane representative of current fighter designs as regards mass and dimensions (table I). Various combinations of derivatives tried are presented in table II, and the coefficients of the quintic equations for these combinations are shown in table III in terms of C_{n_β} and C_{l_β}. Stability diagrams in the form of C_{n_β} plotted against C_{l_β} are given in figures 3 to 9. By following the usual procedures in stability-analysis work, the constant term in the characteristic equation (the coefficient C_6) equated to zero is plotted as the divergence boundary (where one or more of the real roots becomes positive); also, the limiting condition of the three forms of Routh's

discriminant, shown in equation (3), equated to zero is plotted as the oscillatory divergent boundary (real root negative, but a pair of the complex roots positive for all cases investigated). When the constant term in the quintic (the coefficient C_6) becomes negative, the motion is divergent; and when the limiting form of Routh's discriminant becomes negative, the motion has oscillatory instability.

The technique utilized in the solution of motions after application of forcing functions is explained in appendix A.

RESULTS AND DISCUSSION

Stability Diagrams

Cases A and B were computed to show the effect of different rotational rates on the stability boundaries. The rates chosen for cases A and B are similar to those that could be obtained in flat spins, where the rate chosen for case A (r_o = 1.9 radians/sec) would be somewhat slower than the average spin and the rate chosen for case B (r_o = 3.14 radians/sec) would be about normal. For these two cases, plotted as figures 3 and 4 respectively, the damping in roll C_{l_p} was chosen as a reasonable value for a swept-wing airplane based on the oscillation tests presented in reference 6. From previous experience and from oscillation tests presented in reference 6, the values chosen for C_{m_q}, C_{m_θ}, and C_{n_r} are considered to be within the range obtainable, on such a configuration, in the flat-spin region. Figures 3 and 4 indicate the following for cases A and B:

For the slower spin rate (case A) the airplane has oscillatory instability for a range of small negative values of C_{l_β} and for all positive values of C_{l_β}; also, for all positive values of C_{l_β} larger than approximately 0.05, the motion is divergent. For the faster spin rate (case B), both instability boundaries are moved farther into the positive C_{l_β} range. In both instances the instability regions are primarily functions of C_{l_β}. This would seem logical inasmuch as I_Z is about 10 times as large as I_X for the airplane considered. (See table I.) Cases A and B in figures 3 and 4, respectively, show, then, that an increase in the rotational rate could make an airplane having a negative value of C_{l_β} near zero change from a condition for which the flat spin would be

unstable to one in which a stable flat spin would be obtained. This effect on the spin stability of increasing the rotational rate has also been observed on dynamic models tested in the Langley 20-foot free-spinning tunnel.

Cases C and D when compared with cases A and B show the effect of a very small negative value of C_{l_p} (-0.01) on the stability boundaries. For the slower rotational rate (case C, fig. 5), the region of oscillatory instability includes most of the negative C_{l_β} range, whereas the divergence boundary is relatively unaffected by the change in C_{l_p}. Doubling the rotational rate (case D, fig. 6) made motions for given values of negative C_{l_β} stable, whereas they were unstable for case C.

Cases E to G (table III) were investigated to determine what effect a small positive value of C_{l_p} (0.025) might have on the stability of the spin. The original values assumed for C_{m_q} and C_{n_r} lead to a stability equation which indicated, by inspection, that the system would be unstable. (The C_2 coefficient in the stability equation (eq. (A21), which contains the damping terms was negative.) Accordingly, larger negative values for C_{m_q} and C_{n_r} were assumed. The stability plots for cases E to G are presented as figures 7, 8, and 9, respectively, and indicate that instability generally exists for the whole region plotted. As noted by comparing case E with case F, doubling the spin rate r_o and doubling the damping in yaw C_{n_r} caused an extremely small region of stability to occur where originally no stability existed. Flattening the slope of the pitching-moment curve (decreasing C_{m_θ}) had little effect on the stability region obtained for the higher rotational rate. (Compare cases F and G in figs. 8 and 9, respectively.)

On the basis of the results discussed so far, it appears that, for an airplane that is loaded predominantly along the fuselage (as in the present case), a positive value of C_{l_β} in the high-angle-of-attack range will tend to prevent stable flat-spinning conditions. For such a design, it would be expected that the oscillatory instabilities indicated for cases A to G would be evidenced as roll oscillations since the axis of the least inertia is the roll axis.

In order to show the effects of mass distribution on the stability of the flat spin, a case (case H) similar to case B was computed except

that the moments of inertia about the X- and Y-axes were interchanged. Comparison of cases B and H indicates that, although stability existed for negative values of C_{l_β} when the mass was distributed along the fuselage (case B), oscillatory instability is obtained for the whole range of positive and negative values of C_{l_β} when the mass was distributed along the wings. No boundaries are shown in this case (case H) because they fell outside the chosen range of C_{l_β}. This latter condition is undoubtedly attributable to the fact that damping in pitch C_{m_q} was zero. It is probably safe to say that the oscillatory instabilities that exist for case H are pitching oscillations, inasmuch as the axis of the least inertia is the pitch axis. Spin-model tests have also shown that for models loaded predominantly along the wings, the motion is characterized by pitching oscillations. One conclusion that may be drawn from case H is that, for a configuration having its mass predominantly along the wings, a value of C_{n_r} of not less than approximately -0.10, and very little damping in pitch, stable flat-spin conditions will probably not be obtainable at the flat-spin attitudes.

Computed Motions Due to Application of a Forcing Function

Although the limiting assumptions in deriving equations (A26), (A27), and (A28) are such that computation of the motion, after the application of any given disturbance, applies only for small changes from the initial-spin equilibrium position, it was felt that the trends indicated would be in the proper sense; therefore, several computations were made. Because of the limitations of this method the time scale has been kept down to 20 seconds.

It appears that the most effective way to influence the spin and to bring about recovery (according to refs. 4 and 7) is to obtain a yawing moment by applying a moment about an axis which offers the least resistance to a change in angular velocity (least moment of inertia). Accordingly, computed motions were made for applied rolling moments only. These computations were arbitrarily made for cases A, B, and E and are presented in appendix B.

The majority of the cases computed apply to case A in table II and figure 3 $\left(C_{l_p} = -0.10 \text{ and } r_o = 1.9 \text{ radians/sec}\right)$. The motions computed for the stable case (point 1 in fig. 3) show that with $C_{n_\beta} = 0.10$ and

$C_{l_\beta} = -0.15$ when the incremental rolling moment $\frac{\Delta M_X}{I_X}$ originally applied to balance C_{l_p} was removed, the following occurred: The spin rate decreased slightly, θ became slightly more negative (α decreased slightly), and β was slightly changed. (See fig. 10.) It should be noted that removal of the incremental rolling moment $\frac{\Delta M_X}{I_X}$ in this case is equivalent to applying ailerons slightly against the spin, and it appeared unusual that ailerons against the spin would slow down the spin rate or decrease the angle of attack even slightly for the type of mass loading considered. The motion computed for the stable point 2 in figure 3 where C_{n_β} was taken as -0.10 with C_{l_β} still equivalent to -0.15 showed that, for the same type of forcing function used for point 1 (that is, the equivalent of a small aileron deflection against the spin), the spin rate now accelerated somewhat, the angle of attack increased slightly ($\Delta\theta$ slightly positive), and the angle of sideslip became slightly negative. Further, when a rolling-moment coefficient of 0.01, which was assumed equivalent to moving ailerons full with the spin, was applied for point 2, the combined effects of C_{l_p} and ailerons full with the spin indicated a slowing of the spin rate $\left(\frac{dr}{dt} = -0.041 \text{ radian/sec}\right)$, a decrease in the angle of attack $\left(\frac{d\theta}{dt} = -0.002 \text{ radian/sec}\right)$, and positive angle of sideslip ($\beta \approx 2.9^\circ$). (See fig. 11). These effects obtained for point 2 where C_{n_β} was equivalent to -0.10 are consistent with the effects that would usually be anticipated; whereas the effects obtained for point 1 where C_{n_β} was equivalent to 0.10 are inconsistent with the effects that would usually be anticipated.

These differences can be explained on the basis of physical considerations and also from an examination of equations (A1), (A2), and (A3). Physically, it would be anticipated that, for the type of loading considered, the cross-couple inertia yawing moment $(I_X - I_Y)pq$ would act in a sense that would slow down the rotational rate when ailerons are placed with the spin (refs. 6 and 7) or when a positive rolling moment is applied. Similarly, a negative rolling moment (ailerons against the spin) acts in an opposite manner. In addition, if the spin rate slows down, the angle of attack would be expected to decrease because the amount of positive pitching moment supplied by the inertia pitching-moment term $(I_Z - I_X)pr$ would be decreased.

Thus, based on inertia considerations alone, it would be anticipated that a positive rolling moment (ailerons with the spin) would slow down the spin rate and decrease the angle of attack, with the converse holding true for a negative rolling moment. On the other hand, when the aerodynamic yawing-moment characteristics are considered, it would appear that, if a spinning airplane had a positive value of C_{n_β}, movement of ailerons with the spin would cause the inner wing to drop (right wing in a right spin) and permit the airplane to acquire a certain amount of positive sideslip. This combination of positive sideslip combined with positive values of C_{n_β} would cause the airplane to yaw into the spin, that is, to increase the rotational rate. This effect, then, is just opposite to the inertia yawing moment produced by the ailerons. Thus, as C_{n_β} increases from zero in the positive direction, there would apparently be some value of positive C_{n_β} where the aerodynamic and inertia effects would be nullified; and for further increases in positive C_{n_β}, the effects of the ailerons in producing recovery would be reversed.

Examination of the stability equation (eq. (A19)) and equations (A26), (A27), and (A28) for the roll forcing function enables the computation of this point of reversal for the cases considered. These equations indicate that, for the stable-spin cases considered, the most important terms are the coefficients C_5 and C_6 of the stability equation (eq. (A19)) and the constant term in the roll forcing equation. The coefficients C_5 and C_6 are, of course, both positive for the stable cases; and since examination of the roots indicates that the only real root is small, λ, the equations for Δr and $\Delta\theta$ (eqs. (A26) and (A27), respectively) for a stable point when a positive C_l is applied can be simplified roughly to

$$\Delta r = \frac{K_{\Delta r}\left(\frac{I_X - I_Y}{I_Z} r_o^2 \theta_o - \frac{M_{Z_\beta}}{I_Z}\right)}{C_6} - \frac{K_{\Delta r}\left(\frac{I_X - I_Y}{I_Z} r_o^2 \theta_o - \frac{M_{Z_\beta}}{I_Z}\right) e^{\lambda t}}{\lambda C_5} \tag{4}$$

$$\Delta\theta = \frac{K_{\Delta\theta}\left(\frac{I_X - I_Y}{I_Z} r_o^2 \theta_o - \frac{M_{Z_\beta}}{I_Z}\right)}{C_6} - \frac{K_{\Delta\theta}\left(\frac{I_X - I_Y}{I_Z} r_o^2 \theta_o - \frac{M_{Z_\beta}}{I_Z}\right) e^{\lambda t}}{\lambda C_5} \tag{5}$$

where $K_{\Delta r}$ is a negative number, $K_{\Delta\theta}$ is a positive number, and θ_o, according to the original assumption, is a small negative angle. Thus, the value of M_{Z_β} $\left(\text{or } C_{n_\beta}\right)$ for which application of a rolling moment will have no effect on the yawing rate is computed by equating

$$\frac{I_X - I_Y}{I_Z} r_o^2 \theta_o - \frac{M_{Z_\beta}}{I_Z} = 0 \tag{6}$$

For case A, this value of C_{n_β} is 0.055. It is obviously desirable, then, that for the application of a positive rolling moment (ailerons with the spin) to have the greatest effect in producing recovery for the type of loading considered (mass predominantly in the fuselage), C_{n_β} should be a large negative number. (It should be noted that, for a loading in which the mass is extended primarily along the wings, C_{n_β} should be positive.) It should be pointed out that these values of C_{n_β} are favorable for instability, which is good in the spin but is not good for stability in normal flight. Examination of the roll equations (eqs. (A26), (A27), and (A28)) indicates that the wing will always roll in such a manner that the sideslip angle acquired is in the same sense as the rolling moment (that is, a positive C_l leads to a positive β). The value of C_{n_β} just computed for which the reversal of aileron effect occurs also holds in the oscillatory instability region. It is interesting to note that incremental negative values of C_{n_β} due to the fuselage would, in general, be expected when a fuselage nose is providing a damping moment in the spin; whereas positive incremental values of C_{n_β} would probably be present for cases in which the nose is providing a propelling moment.

Motions for points 3 and 4 in the oscillatory instability and divergent regions, respectively, for case A (fig. 3) showed that, for the point in the oscillatory instability region (point 3), Δr would be exceedingly high before any appreciable instability in β would be obvious; whereas the point chosen in the divergent region (point 4) diverged about all three axes almost immediately. (See figs. 12 and 13.) In order to note any divergence in β for the oscillatory instability region, C_{n_β} should be close to 0.055, the point where application of a rolling moment would have no effect on the yawing rate r or on the

angle of attack $(90^\circ + \theta)$. Although the roots were not computed for this case, it is fairly obvious that there would be little change in the roots provided C_{l_β} remained fixed (that is, point 3 increased positively to $C_{n_\beta} = 0.055$ in fig. 3). Then, for a point in the oscillatory instability region of case A (fig. 3) where $C_{l_\beta} = 0$ and $C_{n_\beta} = 0.055$, the motion for the case wherein ailerons are placed full against the spin (C_{l_p} acting and $C_l = -0.01$) would be approximately as shown in figure 14. As is shown, this is a very slow divergence but motions of this nature are often seen in the Langley 20-foot free-spinning tunnel.

A few computations were made for comparison of the motions for the various points numbered 1 ($C_{l_\beta} = -0.15$ and $C_{n_\beta} = 0.1$) for cases A, B, and E and show the effect of increasing the rotational rate and of changing C_{l_p} from a stabilizing value (-0.10) to a destabilizing one (0.025). The most obvious effect for the increased rotation rate is that the response to a rolling moment is in the sense anticipated in that a positive rolling moment decreases the yawing rate. (See fig. 15.) This happens because the value of C_{n_β} for which the effectiveness of the ailerons reverses is increased positively from 0.055 for the slower rate of rotation to 0.155 for the present rate of rotation. The motion for point 1 of case E is now unstable (whereas a stable condition existed for case A), and the motions plotted in figure 16 show that the instability in sideslip is obvious in a short period of time.

The effect of applying a positive pitching moment is as follows: The change in yawing rate Δr is decreased if M_{X_p} is negative unless C_{n_β} becomes sufficiently positive that $\frac{I_X - I_Y}{I_Z} r_o^2 \theta_o - \frac{M_{Z_\beta}}{I_Z}$ becomes negative, β becomes positive provided M_{X_p} is negative, and $\Delta\theta$ is dependent upon various factors and will be positive or negative depending upon whether the following expression is positive or negative:

$$\left[\frac{r_o^2 M_{Z_r}}{I_Z}\left(\frac{I_Y - I_Z}{I_X}\right) + \frac{M_{Z_r}}{I_Z}\frac{M_{X_\beta}}{I_X} - r_o^2\theta_o^2\frac{M_{X_p}}{I_X}\left(\frac{I_X - I_Y}{I_Z}\right) + \frac{M_{X_p}}{I_X}\frac{M_{Z_\beta}}{I_Z}\theta_o\right] \quad (7)$$

Equations (A32) to (A34) show the application of a pitching moment.

The effect of applying a negative yawing moment is as follows: The change in yawing rate Δr is usually decreased and a negative yawing moment has the greatest effect in reducing Δr if M_{X_β} and M_{X_p} are large negative values, β generally becomes negative if M_{X_p} is negative, and $\Delta\theta$ becomes more negative (α decreases) unless $\frac{M_{X_\beta}}{I_X}$ becomes large enough positively to exceed $\frac{I_Y - I_Z}{I_X} r_o^2$. (See eqs. (A29) to (A31) for application of a yawing moment.)

Thus, application of a positive pitching moment appears to produce an effect similar to the application of a positive rolling moment as regards its effect on reducing the spin rate, and a negative yawing moment also reduces the spin rate. These effects are consistent with effects observed from experimental spin research in the Langley 20-foot free-spinning tunnel.

A few calculations have been made on a high-speed digital computer, utilizing six-degree-of-freedom equations of motion, in an attempt to check the validity of the results presented in this paper. Although some limiting assumptions had to be made in carrying out the six-degree-of-freedom studies, the results are considered to indicate the qualitative validity of the three-degree-of-freedom results in this paper.

CONCLUSIONS

The following conclusions are based on linearized equations of motion utilizing only the three moment equations and assuming only flat-spin conditions:

1. Contemporary airplane designs (with the moment of inertia about the wing axis I_Y considerably greater than the moment of inertia about the fuselage axis I_X) having positive values of rolling-moment coefficient due to rolling or rolling-moment coefficient due to sideslip will probably not have a stable spin near an angle of attack of 90°. In addition, high rotational rates have a stabilizing effect on flat spins, an effect which has been observed during spin-model tests in the Langley 20-foot free-spinning tunnel.

2. If the damping in pitch in flat-spin attitudes is zero, it would not be possible to obtain stable flat spins if the moments of inertia of

the airplane are such that the mass is primarily distributed along the wings, that is, with I_X considerably greater than I_Y (opposite to the mass distribution of contemporary fighter designs).

3. The effect of moving ailerons with the spin in producing recovery for contemporary fighter designs will be greatest for large negative values of yawing-moment coefficient due to sideslip C_{n_β}, and for a certain critical value of positive C_{n_β} the rolling moment applied by moving ailerons with the spin will have no effect on reducing the spin rate. These effects also apply to an application of a positive pitching moment.

Langley Research Center,
National Aeronautics and Space Administration,
Langley Field, Va., February 25, 1959.

APPENDIX A

DERIVATIONS OF EQUATIONS

Equations for Determining Stability Boundary

The equations of motion corresponding to the rolling, pitching, and yawing degrees of freedom are, respectively,

$$\text{Roll} = I_X\dot{p} = \left(I_Y - I_Z\right)qr + M_{X_\beta}\beta + M_{X_p}p + \Delta M_X \tag{A1}$$

$$\text{Pitch} = I_Y\dot{q} = \left(I_Z - I_X\right)pr + M_{Y_\theta}\theta + M_{Y_q}q + M_{Y,o} \tag{A2}$$

$$\text{Yaw} = I_Z\dot{r} = \left(I_X - I_Y\right)pq + M_{Z_r}r + M_{Z_\beta}\beta + \Delta M_Z \tag{A3}$$

Expressing the angular velocities about the body axes in terms of the (Euler's) attitude angles gives

$$p = \dot{\phi} - \dot{\psi}\sin\theta \tag{A4}$$

$$q = \dot{\theta}\cos\phi + \dot{\psi}\cos\theta\sin\phi \tag{A5}$$

$$r = -\dot{\theta}\sin\phi + \dot{\psi}\cos\theta\cos\phi \tag{A6}$$

(See appendix A in ref. 8, for example.) The following assumptions were applied:

$$\theta = \theta_o + \Delta\theta$$

$$\dot{\psi} = r_o + \Delta r$$

$$\beta = \phi = \beta_o + \Delta\beta \qquad \left(\beta_o = 0\right)$$

$$\sin\angle = \angle$$

$$\cos\angle = 1$$

Rewriting equations (A4), (A5), and (A6) with the aforementioned assumptions included and with second-order terms neglected gives, respectively,

$$p = \Delta\dot{\beta} - r_o\theta_o - r_o\,\Delta\theta - \theta_o\,\Delta r \tag{A7}$$

$$q = \Delta\dot{\theta} + r_o\,\Delta\beta \tag{A8}$$

$$r = r_o + \Delta r \tag{A9}$$

which can be expressed as

$$\dot{p} = \Delta\ddot{\beta} - r_o\,\Delta\dot{\theta} - \theta_o\,\Delta\dot{r} \tag{A10}$$

$$\dot{q} = \Delta\ddot{\theta} + r_o\,\Delta\dot{\beta} \tag{A11}$$

$$\dot{r} = \Delta\dot{r} \tag{A12}$$

or as

$$pr = r_o\,\Delta\dot{\beta} - 2r_o\theta_o\,\Delta r - r_o^2\Delta\theta - r_o^2\theta_o \tag{A13}$$

$$pq = -r_o\theta_o\,\Delta\dot{\theta} - r_o^2\theta_o\,\Delta\beta \tag{A14}$$

$$qr = r_o\,\Delta\dot{\theta} + r_o^2\Delta\beta \tag{A15}$$

Substituting equations (A7) to (A15) into equations (A1) to (A3) and neglecting second-order terms gives the three moment equations in the following form: Roll is given as

$$\text{Roll} = \Delta\beta\left[D^2 - \frac{M_{X_p}}{I_X}D - \left(\frac{I_Y - I_Z}{I_X}r_o^2 + \frac{M_{X_\beta}}{I_X}\right)\right] +$$

$$\Delta\theta\left[-r_o\left(1 + \frac{I_Y - I_Z}{I_X}\right)D + \frac{M_{X_p}}{I_X}r_o\right] + \Delta r\left[-\theta_o D + \frac{M_{X_p}}{I_X}\theta_o\right]$$

$$= -\frac{M_{X_p}}{I_X}r_o\theta_o + \frac{\Delta M_X}{I_X} \tag{A16}$$

where $-\frac{M_{X_p}}{I_X} r_o\theta_o$ and $\frac{\Delta M_X}{I_X}$ cancel each other for balance at $\beta = 0^o$ for the initial steady spin. Pitch is given as

$$\text{Pitch} = \Delta\beta\left[r_o\left(1 - \frac{I_Z - I_X}{I_Y}\right)D - \frac{M_{Y_q}}{I_Y} r_o\right] +$$

$$\Delta\theta\left[D^2 - \frac{M_{Y_q}}{I_Y} D + \left(\frac{I_Z - I_X}{I_Y} r_o^2 - \frac{M_{Y_\theta}}{I_Y}\right)\right] +$$

$$\Delta r\left[2r_o\theta_o \frac{I_Z - I_X}{I_Y}\right]$$

$$= \frac{M_Y}{I_Y} - r_o^2\theta_o \frac{I_Z - I_X}{I_Y} + \frac{M_{Y_\theta}}{I_Y}\theta_o + \frac{M_{Y,o}}{I_Y} \qquad \text{(A17)}$$

where $\frac{M_Y}{I_Y}$ is considered to be equivalent to zero for the initial steady spin and $\left(-r_o^2\theta_o \frac{I_Z - I_X}{I_Y} + \frac{M_{Y_\theta}}{I_Y}\theta_o + \frac{M_{Y,o}}{I_Y}\right)$ cancel each other for balance for the steady-spin state. Yaw is given as

$$\text{Yaw} = \Delta\beta\left[\frac{I_X - I_Y}{I_Z} r_o^2\theta_o - \frac{M_{Z_\beta}}{I_Z}\right] + \Delta\theta\left[\frac{I_X - I_Y}{I_Z} r_o\theta_o D\right] + \Delta r\left[D - \frac{M_{Z_r}}{I_Z}\right]$$

$$= \frac{M_{Z_r}}{I_Z} r_o + \frac{\Delta M_Z}{I_Z} \qquad \text{(A18)}$$

where $\frac{M_{Z_r}}{I_Z} r_o$ and $\frac{\Delta M_Z}{I_Z}$ cancel each other for balance for the initial steady spin.

By placing equations (A16), (A17), and (A18) in determinate form and solving for the characteristic equation, an equation of the following form is obtained:

$$C_1 D^5 + C_2 D^4 + C_3 D^3 + C_4 D^2 + C_5 D + C_6 = 0 \tag{A19}$$

where the coefficients of the characteristic equation are given as

$$C_1 = 1 \tag{A20}$$

$$C_2 = - \frac{M_{X_p}}{I_X} - \frac{M_{Y_q}}{I_Y} - \frac{M_{Z_r}}{I_Z} \tag{A21}$$

$$C_3 = - \frac{M_{X_\beta}}{I_X} + \frac{M_{X_p}}{I_X} \frac{M_{Y_q}}{I_Y} - \frac{M_{Y_\theta}}{I_Y} + \frac{M_{Z_r}}{I_Z} \frac{M_{X_p}}{I_X} + \frac{M_{Z_r}}{I_Z} \frac{M_{Y_q}}{I_Y} - \frac{M_{Z_\beta}}{I_Z} \theta_o +$$

$$\left[1 - \left(\frac{I_Y - I_Z}{I_X}\right)\left(\frac{I_Z - I_X}{I_Y}\right)\right] r_o^2 - r_o^2 \theta_o^2 \left(\frac{I_Z - I_X}{I_Y}\right)\left(\frac{I_X - I_Y}{I_Z}\right) \tag{A22}$$

$$C_4 = \frac{M_{Y_q}}{I_Y} \frac{M_{X_\beta}}{I_X} + \frac{M_{Y_\theta}}{I_Y} \frac{M_{X_p}}{I_X} + \frac{M_{X_\beta}}{I_X} \frac{M_{Z_r}}{I_Z} - \frac{M_{X_p}}{I_X} \frac{M_{Y_q}}{I_Y} \frac{M_{Z_r}}{I_Z} + \frac{M_{Z_r}}{I_Z} \frac{M_{Y_\theta}}{I_Y} + \frac{M_{Y_q}}{I_Y} \frac{M_{Z_\beta}}{I_Z} \theta_o +$$

$$\frac{M_{Z_\beta}}{I_Z} \frac{M_{X_p}}{I_X} \theta_o - \frac{M_{X_p}}{I_X} r_o^2 - \frac{M_{Y_q}}{I_Y} r_o^2 - \frac{M_{Z_r}}{I_Z} r_o^2 \left[1 - \left(\frac{I_Y - I_Z}{I_X}\right)\left(\frac{I_Z - I_X}{I_Y}\right)\right] +$$

$$r_o^2 \theta_o^2 \frac{M_{X_p}}{I_X} \left(\frac{I_Z - I_X}{I_Y}\right)\left(\frac{I_X - I_Y}{I_Z}\right) \tag{A23}$$

$$C_5 = - r_o^4\left(\frac{I_Y - I_Z}{I_X}\right)\left(\frac{I_Z - I_X}{I_Y}\right) - r_o^2\,\frac{M_{X_\beta}}{I_X}\left(\frac{I_Z - I_X}{I_Y}\right) + r_o^2\,\frac{M_{Y_\theta}}{I_Y}\left(\frac{I_Y - I_Z}{I_X}\right) +$$

$$\frac{M_{Y_\theta}}{I_Y}\frac{M_{X_\beta}}{I_X} - \frac{M_{Y_q}}{I_Y}\frac{M_{X_\beta}}{I_X}\frac{M_{Z_r}}{I_Z} - \frac{M_{Y_\theta}}{I_Y}\frac{M_{X_p}}{I_X}\frac{M_{Z_r}}{I_Z} - r_o^4\theta_o^2\left(\frac{I_Z - I_X}{I_Y}\right)\left(\frac{I_X - I_Y}{I_Z}\right) +$$

$$2r_o^2\theta_o\,\frac{M_{Z_\beta}}{I_Z}\left(\frac{I_Z - I_X}{I_Y}\right)\left(\frac{1}{2} + \frac{I_Y - I_Z}{I_X}\right) + \frac{M_{Z_\beta}}{I_Z}\frac{M_{Y_\theta}}{I_Y}\,\theta_o - \frac{M_{Y_\theta}}{I_Y}\left(\frac{I_X - I_Y}{I_Z}\right) r_o^2\theta_o^2 -$$

$$\frac{M_{Y_q}}{I_Y}\frac{M_{Z_\beta}}{I_Z}\frac{M_{X_p}}{I_X}\,\theta_o + \frac{M_{Y_q}}{I_Y}\frac{M_{X_p}}{I_X}\,r_o^2 + \frac{M_{Z_r}}{I_Z}\frac{M_{X_p}}{I_X}\,r_o^2 + \frac{M_{Y_q}}{I_Y}\frac{M_{Z_r}}{I_Z}\,r_o^2 +$$

$$2r_o^2\theta_o^2\,\frac{M_{X_\beta}}{I_X}\left(\frac{I_X - I_Y}{I_Z}\right)\left(\frac{I_Z - I_X}{I_Y}\right) \qquad \text{(A24)}$$

$$C_6 = r_o^4\left(\frac{I_Y - I_Z}{I_X}\right)\left(\frac{I_Z - I_X}{I_Y}\right)\frac{M_{Z_r}}{I_Z} + r_o^2\left(\frac{I_Z - I_X}{I_Y}\right)\frac{M_{X_\beta}}{I_X}\frac{M_{Z_r}}{I_Z} -$$

$$r_o^2\,\frac{M_{Y_\theta}}{I_Y}\left(\frac{I_Y - I_Z}{I_X}\right)\frac{M_{Z_r}}{I_Z} - \frac{M_{Y_\theta}}{I_Y}\frac{M_{X_\beta}}{I_X}\frac{M_{Z_r}}{I_Z} - r_o^2\theta_o\,\frac{M_{X_p}}{I_X}\frac{M_{Z_\beta}}{I_Z}\left(\frac{I_Z - I_X}{I_Y}\right) +$$

$$r_o^4\theta_o^2\,\frac{M_{X_p}}{I_X}\left(\frac{I_X - I_Y}{I_Z}\right)\left(\frac{I_Z - I_X}{I_Y}\right) + \frac{M_{Y_\theta}}{I_Y}\frac{M_{X_p}}{I_X}\left(\frac{I_X - I_Y}{I_Z}\right) r_o^2\theta_o^2 -$$

$$\frac{M_{Y_\theta}}{I_Y}\frac{M_{Z_\beta}}{I_Z}\frac{M_{X_p}}{I_X}\,\theta_o - \frac{M_{Z_r}}{I_Z}\frac{M_{Y_q}}{I_Y}\frac{M_{X_p}}{I_X}\,r_o^2 \qquad \text{(A25)}$$

Equations for Solution of Motion After Application of Various Forcing Functions

In order to solve for the motion after various forcing functions were applied, the five roots of the characteristic equations were determined as were the differential equations for the various forcing functions. The solution for any of the motions $\Delta\theta$, Δr, or $\Delta\beta$ is then determined from

$$\Delta\theta, \quad \Delta r, \text{ or } \quad \Delta\beta = \frac{f(d)}{F(d)}$$

where $f(d)$ is the numerator of the equation for the motion after various forcing functions are applied and $F(d)$ is the characteristic equation. The forcing functions employed were step inputs for which Heaviside's expansion could be employed to obtain a solution

$$\Delta\theta, \quad \Delta r, \text{ or } \quad \Delta\beta = \frac{f(0)}{F(0)} + \sum \frac{f(\lambda)}{\lambda F'(\lambda)} e^{\lambda t}$$

where the various values of λ are the five roots of the characteristic equation and F' indicates the first derivative of the characteristic equation. In order to solve this equation for the complex roots, the method explained in reference 9 was employed. The equations for the motion after application of various forcing functions and the removal of the $\frac{\Delta M_X}{I_X}$ term originally inserted intc equation (A16) for balance at zero sideslip are as follows:

$$\Delta r = \frac{M_{X_p}}{I_X} r_o\theta_o \left[\left(r_o^2\theta_o \frac{I_X - I_Y}{I_Z} \frac{I_Z - I_X}{I_Y} - \frac{M_{Z_\beta}}{I_Z} \right) D^2 + \frac{M_{Y_q}}{I_Y} \frac{M_{Z_\beta}}{I_Z} D + \left(\frac{I_Z - I_X}{I_Y} r_o^2 - \frac{M_{Y_\theta}}{I_Y} \right) \left(\frac{I_X - I_Y}{I_Z} r_o^2\epsilon_o - \frac{M_{Z_\beta}}{I_Z} \right) \right] \frac{1}{F(d)} \tag{A26}$$

$$\Delta\theta = \frac{M_{X_p}}{I_X} r_o\theta_o \left[r_o\left(1 - \frac{I_Z - I_X}{I_Y}\right)D^2 + \left(- \frac{M_{Y_q}}{I_Y} r_o - \frac{M_{Z_r}}{I_Z} r_o \right)\left(1 - \frac{I_Z - I_X}{I_Y}\right)D + \left(\frac{M_{Y_q}}{I_Y} \frac{M_{Z_r}}{I_Z} r_o - 2r_o^3\theta_o^2 \frac{I_X - I_Y}{I_Z} \frac{I_Z - I_X}{I_Y} + 2r_o\theta_o \frac{M_{Z_\beta}}{I_Z} \frac{I_Z - I_X}{I_Y} \right) \right] \frac{1}{F(d)} \tag{A27}$$

$$\Delta\beta = \frac{M_{X_p}}{I_X} r_o\theta_o \left[-D^3 + \left(\frac{M_{Y_q}}{I_Y} + \frac{M_{Z_r}}{I_Z} \right)D^2 + \left(- \frac{I_Z - I_X}{I_Y} r_o^2 + \frac{M_{Y_\theta}}{I_Y} - \frac{M_{Z_r}}{I_Z} \frac{M_{Y_q}}{I_Y} + 2r_o^2\theta_o^2 \frac{I_X - I_Y}{I_Z} \frac{I_Z - I_X}{I_Y} \right)D + \frac{M_{Z_r}}{I_Z} \left(\frac{I_Z - I_X}{I_Y} r_o^2 - \frac{M_{Y_\theta}}{I_Y} \right) \right] \frac{1}{F(d)} \tag{A28}$$

Application of a rolling moment.- After the application of a rolling moment the equations for Δr, $\Delta\theta$, and $\Delta\beta$ are the same as those given in equations (A26), (A27), and (A28), respectively, except that the $\frac{M_{X_p}}{I_X} r_o\theta_o$ term is replaced by $- \frac{\Delta M_X}{I_X}$.

Application of a yawing moment.- After the application of a yawing moment the equations for Δr, $\Delta\theta$, and $\Delta\beta$ are given, respectively, as

$$\Delta r = \frac{M_Z}{I_Z}\left[D^4 - \left(\frac{M_{X_p}}{I_X} + \frac{M_{Y_q}}{I_Y}\right)D^3 + \left(\frac{M_{X_p}}{I_X}\frac{M_{Y_q}}{I_Y} - \frac{M_{X_\beta}}{I_X} - \frac{M_{Y_\theta}}{I_Y} + r_o^2\left\{1 - \frac{I_Z - I_X}{I_Y}\frac{I_Y - I_Z}{I_X}\right\}\right)D^2 + \left(\frac{M_{X_\beta}}{I_X}\frac{M_{Y_q}}{I_Y} + \frac{M_{Y_\theta}}{I_Y}\frac{M_{X_p}}{I_X} - r_o^2\frac{M_{Y_q}}{I_Y} - r_o^2\frac{M_{X_p}}{I_X}\right)D + r_o^2\frac{M_{X_p}}{I_X}\frac{M_{Y_q}}{I_Y} + \frac{M_{Y_\theta}}{I_Y}\frac{I_Y - I_Z}{I_X}r_o^2 - \frac{I_Y - I_Z}{I_X}\frac{I_Z - I_X}{I_Y}r_o^4 - \frac{M_{X_\beta}}{I_X}\frac{I_Z - I_X}{I_Y}r_o^2 + \frac{M_{Y_\theta}}{I_Y}\frac{M_{X_\beta}}{I_X}\right]\frac{1}{F(d)} \tag{A29}$$

$$\Delta\theta = \frac{M_Z}{I_Z}\theta_o r_o\left[\left(-1 - \frac{I_Z - I_X}{I_Y}\right)D^2 + \left(\frac{M_{Y_q}}{I_Y} + \frac{M_{X_p}}{I_X} + \frac{M_{X_p}}{I_X}\frac{I_Z - I_X}{I_Y}\right)D + 2\frac{I_Z - I_X}{I_Y}\left(\frac{I_Y - I_Z}{I_X}r_o^2 + \frac{M_{X_\beta}}{I_X}\right) - \frac{M_{Y_q}}{I_Y}\frac{M_{X_p}}{I_X}\right]\frac{1}{F(d)} \tag{A30}$$

$$\Delta\beta = \frac{M_Z}{I_Z}\theta_o\left[D^3 - \left(\frac{M_{Y_q}}{I_Y} + \frac{M_{X_p}}{I_X}\right)D^2 + \left(-\frac{I_Z - I_X}{I_Y}r_o^2 - 2\frac{I_Z - I_X}{I_Y}\frac{I_Y - I_Z}{I_X}r_o^2 + \frac{M_{X_p}}{I_X}\frac{M_{Y_q}}{I_Y} - \frac{M_{Y_\theta}}{I_Y}\right)D + \frac{M_{X_p}}{I_X}\frac{I_Z - I_X}{I_Y}r_o^2 + \frac{M_{X_p}}{I_X}\frac{M_{Y_\theta}}{I_Y}\right]\frac{1}{F(d)} \tag{A31}$$

Application of a pitching moment.- After the application of a pitching moment, the equations for Δr, $\Delta\theta$, and $\Delta\beta$ are given, respectively, as

$$\Delta r = \frac{M_Y}{I_Y}\left\{\left(-r_o\theta_o\frac{I_X - I_Y}{I_Z}\right)D^3 + \left(r_o\theta_o\frac{M_{X_p}}{I_X}\frac{I_X - I_Y}{I_Z}\right)D^2 + \left[r_o\theta_o\frac{M_{X_\beta}}{I_X}\frac{I_X - I_Y}{I_Z} - r_o{}^3\theta_o\frac{I_X - I_Y}{I_Z} + r_o\frac{M_{Z_\beta}}{I_Z}\left(1 + \frac{I_Y - I_Z}{I_X}\right)\right]D + r_o{}^3\theta_o\frac{M_{X_p}}{I_X}\frac{I_X - I_Y}{I_Z} - r_o\frac{M_{Z_\beta}}{I_Z}\frac{M_{X_p}}{I_X}\right\}\frac{1}{F(d)} \tag{A32}$$

$$\Delta\theta = \frac{M_Y}{I_Y}\left[D^3 - \left(\frac{M_{X_p}}{I_X} + \frac{M_{Z_r}}{I_Z}\right)D^2 - \left(r_o{}^2\frac{I_Y - I_Z}{I_X} + \frac{M_{X_\beta}}{I_X} - \frac{M_{Z_r}}{I_Z}\frac{M_{X_p}}{I_X} - \theta_o{}^2r_o{}^2\frac{I_X - I_Y}{I_Z} + \frac{M_{Z_\beta}}{I_Z}\theta_o\right)D + r_o{}^2\frac{M_{Z_r}}{I_Z}\frac{I_Y - I_Z}{I_X} + \frac{M_{Z_r}}{I_Z}\frac{M_{X_\beta}}{I_X} - r_o{}^2\theta_o{}^2\frac{M_{X_p}}{I_X}\frac{I_X - I_Y}{I_Z} + \theta_o\frac{M_{X_p}}{I_X}\frac{M_{Z_\beta}}{I_Z}\right]\frac{1}{F(d)} \tag{A33}$$

$$\Delta\beta = \frac{M_Y}{I_Y}r_o\left\{\left(1 + \frac{I_Y - I_Z}{I_X} - \frac{I_X - I_Y}{I_Z}\theta_o{}^2\right)D^2 + \left[\frac{M_{X_p}}{I_X}\frac{I_X - I_Y}{I_Z}\theta_o{}^2 - \frac{M_{X_p}}{I_X} - \frac{M_{Z_r}}{I_Z}\left(1 + \frac{I_Y - I_Z}{I_X}\right)\right]D + \frac{M_{Z_r}}{I_Z}\frac{M_{X_p}}{I_X}\right\}\frac{1}{F(d)} \tag{A34}$$

APPENDIX B

EQUATIONS FOR MOTION OBTAINED WHEN VARIOUS FORCING FUNCTIONS ARE APPLIED IN ROLL

Case A

In the determination of points 1 to 4 in figure 3 for case A, the $\frac{\Delta M_X}{I_X}$ term is removed from equation (A16) which then allows M_{X_p} to act. Thus, Δr, 0θ, and $\Delta\beta$ can be expressed, respectively, as follows:

Point 1 in figure 3.-

$$\Delta r = -0.03903 + 0.039064e^{-0.0267t} + 0.000196e^{-0.01718t}\cos(1.696t + 6.1665) + 0.0000514e^{-0.15045t}\cos(3.328t + 3.6249)$$

$$\Delta\theta = -0.00252 + 0.002521e^{-0.0267t} + 0.00040e^{-0.01718t}\cos(1.696t + 3.09) + 0.0000156e^{-0.15045t}\cos(3.328t + 2.904)$$

$$\Delta\beta = -0.005466 + 0.010736e^{-0.0267t} + 0.000528e^{-0.01718t}\cos(1.696t + 4.606) + 0.001126e^{-0.15045t}\cos(3.328t + 4.647)$$

Point 2 in figure 3.-

$$\Delta r = 0.128656 - 0.128796e^{-0.02925t}$$

$$\Delta\theta = 0.00946 - 0.00947e^{-0.02925t}$$

$$\Delta\beta = -0.004996 - 0.000271e^{-0.02925t}$$

It should be noted that the oscillatory terms were not computed for this case in that they were assumed to be of negligible importance for the time range considered.

If $C_l = 0.01$ is applied, the result is

$$\Delta r = -1.3291 + 1.3305e^{-0.02925t}$$

$$\Delta\theta = -0.09772 + 0.0978e^{-0.02925t}$$

$$\Delta\beta = 0.051648 + 0.002769e^{-0.02925t}$$

Point 3 in figure 3.-

$$\Delta r = 0.5764 - 0.5878e^{-0.035t} + 0.0058e^{-0.17t}\cos(1.32t + 1.37) + 0.00092e^{0.0125t}\cos(2.05t + 0.729)$$

$$\Delta\theta = 0.0424 - 0.0432e^{-0.035t} + 0.00026e^{-0.17t}\cos(1.32t + 0.99) + 0.0001e^{0.0125t}\cos(2.05t + 1.84)$$

$$\Delta\beta = -0.02346 - 0.005e^{-0.035t} + 0.029e^{-0.17t}\cos(1.32t + 6.18) + 0.0004e^{0.0125t}\cos(2.05t + 5.28)$$

If $C_l = -0.01$ is applied, $\Delta\beta$ can be written as

$$\Delta\beta = -0.2438 - 0.0558e^{-0.035t} + 0.1122e^{-0.17t}\cos(1.32t + 6.19) + 0.0027e^{0.0125t}\cos(2.05t + 5.14)$$

Point 4 in figure 3.-

$$\Delta r = -0.05515 + 0.00028e^{2.798t} - 0.00022e^{-3.13t} + 0.05013e^{-0.03t} + 0.00002e^{0.005t}\cos(2.043t + 4.94)$$

$$\Delta\theta = -0.00405 + 0.00007e^{2.798t} - 0.00006e^{-3.13t} + 0.00368e^{-0.03t} +$$

$$0.00013e^{0.005t}\cos(2.043t + 1.621)$$

$$\Delta\beta = 0.00593 - 0.00309e^{2.798t} - 0.00275e^{-3.13t} + 0.00044e^{-0.03t} +$$

$$0.00003e^{0.005t}\cos(2.043t + 5.554)$$

If $C_l = -0.01$ is applied, $\Delta\beta$ can be written as

$$\Delta\beta = -0.05651 + 0.002166e^{-0.0267t} + 0.0348e^{-0.01718t}\cos(1.696t + 6.19) +$$

$$0.03876e^{-0.15045t}\cos(3.328t + 6.26)$$

Case B - Point 1 in Figure 4

In the determination of point 1 in figure 4 for case B, the $\frac{\Delta M_X}{I_X}$ term is removed from equation (A16) to allow M_{X_p} to act. Thus,

$$\Delta r = 0.0597 - 0.0596e^{-0.0273t} + 0.0000274e^{-0.0363t}\cos(3.133t + 4.41) +$$

$$0.000228e^{-0.225t}\cos(3.65t + 1.60)$$

$$\Delta\theta = 0.003 - 0.0029e^{-0.0273t} + 0.00092e^{-0.0363t}\cos(3.133t + 1.18) +$$

$$0.00078e^{-0.225t}\cos(3.65t + 0.78)$$

$$\Delta\beta = -0.0066 + 0.000056e^{-0.0273t} + 0.0005e^{-0.0363t}\cos(3.133t + 2.63) +$$

$$0.0055e^{-0.225t}\cos(3.65t + 6.07)$$

If $C_l = 0.01$ is applied, Δr, $\Delta\theta$, and $\Delta\beta$ (with oscillatory terms being of small importance in determining $\Delta\theta$ and final trim β) are given, respectively, as

$$\Delta r = -0.3782 + 0.3776e^{-0.0273t} + 0.001648e^{-0.0363t}\cos(3.133t + 1.27) +$$

$$0.001442e^{-0.225t}\cos(3.65t + 4.73)$$

$$\Delta\theta = -0.016 + 0.016e^{-0.0273t}$$

$$\Delta\beta = 0.035 + 0.0003e^{-0.0273t}$$

Case E - Point 1 in Figure 7

In the determination of point 1 in figure 7 for case E, the $\frac{\Delta M_X}{I_X}$ term is removed from equation (A16) to allow M_{X_p} to act. Thus,

$$\Delta r = 0.002707 - 0.002703e^{-0.092t} + 0.0000203e^{-0.003t}\cos(2.018t + 4.71) +$$

$$0.000092e^{0.039t}\cos(3.15t + 1.62)$$

$$\Delta\theta = 0.000204 - 0.000208e^{-0.092t} + 0.0001e^{-0.003t}\cos(2.018t + 1.53) +$$

$$0.000067e^{0.039t}\cos(3.15t + 4.71)$$

$$\Delta\beta = 0.00131 - 0.000055e^{-0.092t} + 0.000049e^{-0.003t}\cos(2.018t + 0.04) +$$

$$0.00131e^{0.039t}\cos(3.15t + 3.17)$$

If $C_l = -0.01$ is applied, the result is

$$\Delta r = -0.111864 + 0.111732e^{-0.092t} + 0.00084e^{-0.003t}\cos(2.018t + 1.57) +$$

$$0.0038e^{0.039t}\cos(3.15t + 4.76)$$

$$\Delta\theta = -0.00839 + 0.00856e^{-0.092t} + 0.00472e^{-0.003t}\cos(2.018t + 4.67) + 0.00276e^{0.039t}\cos(3.15t + 1.67)$$

$$\Delta\beta = -0.054337 + 0.002268e^{-0.092t} + 0.00202e^{-0.003t}\cos(2.018t + 3.18) + 0.054256e^{0.039t}\cos(3.15t + 0.01)$$

REFERENCES

1. Neihouse, Anshal I., Klinar, Walter J., and Scher, Stanley H.: Status of Spin Research for Recent Airplane Designs. NACA RM L57F12, 1957.

2. Polhamus, Edward C.: Effect of Flow Incidence and Reynolds Number on Low-Speed Aerodynamic Characteristics of Several Noncircular Cylinders With Applications to Directional Stability and Spinning. NACA TN 4176, 1958.

3. Burk, Sanger M., Jr.: Analytical Determination of the Mechanism of an Airplane Spin Recovery With Different Applied Yawing Moments by Use of Rotary-Balance Data. NACA TN 3321, 1954.

4. Routh, Edward John: Dynamics of a System of Rigid Bodies. Part II. Sixth ed., rev. and enl., MacMillan and Co., Ltd., 1905.

5. Imlay, Frederick H.: A Theoretical Study of Lateral Stability With an Automatic Pilot. NACA Rep. 693, 1940.

6. Johnson, Joseph L., Jr.: Low-Speed Measurements of Static Stability, Damping in Yaw, and Damping in Roll of a Delta, a Swept, and an Unswept Wing for Angles of Attack From 0° to 90°. NACA RM L56B01, 1956.

7. Neihouse, A. I.: A Mass-Distribution Criterion for Predicting the Effect of Control Manipulation on the Recovery From a Spin. NACA WR L-168, 1942. (Formerly NACA ARR, Aug. 1942.)

8. Scher, Stanley H.: An Analytical Investigation of Airplane Spin-Recovery Motion by Use of Rotary-Balance Aerodynamic Data. NACA TN 3188, 1954.

9. Jones, Robert T.: A Simplified Application of the Method of Operators to the Calculation of Disturbed Motions of an Airplane. NACA Rep. 560, 1936.

TABLE I.- MASS AND DIMENSIONAL CHARACTERISTICS OF AIRPLANE

I_X, slug-ft^2	10,000
I_Y, slug-ft^2	110,000
I_Z, slug-ft^2	115,000
S, sq ft	385.33
b, ft	35.7
Test altitude, ft	30,000

TABLE II.- CONDITIONS INVESTIGATED

	Case A	Case B	Case C	Case D	Case E	Case F	Case G	Case H (a)
C_{l_p}	-0.10	-0.10	-0.01	-0.01	0.025	0.025	0.025	0.10
C_{n_r}	-0.10	-0.10	-0.10	-0.10	-0.33	-0.66	-0.66	-0.10
C_{m_q}	0	0	0	0	-0.028	-0.028	-0.028	0
C_{m_θ}	-0.14	-0.14	-0.14	-0.14	-0.14	-0.14	-0.07	-0.14
r_o, radians/sec	1.9	3.14	1.9	3.8	1.9	3.8	3.8	3.14
θ_o, deg	-5	-5	-5	-5	-5	-5	-5	-5
V, ft/sec	297	297	297	297	297	297	297	297

[a]For case H the moments of inertia about the X- and Y-axes are interchanged.

TABLE III.- COEFFICIENTS OF CHARACTERISTIC EQUATION FOR THE CASES INVESTIGATED (SEE TABLE II)

Coefficient	Case A	Case B	Case C
C_1	1	1	1
C_2	0.35	0.35	0.061
C_3	$0.371C_{n_\beta} - 53C_{l_\beta} + 6.022$	$0.371C_{n_\beta} - 53C_{l_\beta} + 15.306$	$0.371C_{n_\beta} - 53C_{l_\beta} + 6.029$
C_4	$0.125C_{n_\beta} - 1.484C_{l_\beta} + 1.620$	$0.125C_{n_\beta} - 1.484C_{l_\beta} + 3.813$	$0.012C_{n_\beta} - 1.484C_{l_\beta} + 0.508$
C_5	$0.260C_{n_\beta} - 219.95C_{l_\beta} + 7.514$	$0.260C_{n_\beta} - 540.826C_{l_\beta} + 50.356$	$0.260C_{n_\beta} - 219.95C_{l_\beta} + 7.501$
C_6	$-0.339C_{n_\beta} - 6.137C_{l_\beta} + 0.229$	$-1.156C_{n_\beta} - 14.875C_{l_\beta} + 1.468$	$-0.032C_{n_\beta} - 5.247C_{l_\beta} + 0.212$

Coefficient	Case D	Case E	Case F
C_1	1	1	1
C_2	0.061	0.02	0.113
C_3	$0.371C_{n_\beta} - 53C_{l_\beta} + 22.090$	$0.371C_{n_\beta} - 53C_{l_\beta} - 6.006$	$0.371C_{n_\beta} - 53C_{l_\beta} + 22.075$
C_4	$0.012C_{n_\beta} - 1.484C_{l_\beta} + 1.112$	$-0.028C_{n_\beta} - 5.353C_{l_\beta} + 0.239$	$-0.028C_{n_\beta} - 10.282C_{l_\beta} + 2.980$
C_5	$0.260C_{n_\beta} - 702.25C_{l_\beta} + 12.554$	$0.265C_{n_\beta} - 220.044C_{l_\beta} + 7.447$	$0.265C_{n_\beta} - 774.94C_{l_\beta} + 105.313$
C_6	$-0.159C_{n_\beta} - 20.67C_{l_\beta} + 0.357$	$0.085C_{n_\beta} - 20.23C_{l_\beta} + 0.685$	$0.408C_{n_\beta} - 142.305C_{l_\beta} + 19.316$

Coefficient	Case G	Case H
C_1	1	1
C_2	0.113	0.057
C_3	$0.371C_{n_\beta} - 53C_{l_\beta} + 21.738$	$0.384C_{n_\beta} - 4.818C_{l_\beta} + 21.957$
C_4	$-0.028C_{n_\beta} - 10.282C_{l_\beta} + 2.944$	$0.011C_{n_\beta} - 0.134C_{l_\beta} + 1.113$
C_5	$0.132C_{n_\beta} - 757.716C_{l_\beta} + 102.913$	$4.569C_{n_\beta} - 59.218C_{l_\beta} + 116.368$
C_6	$0.429C_{n_\beta} - 138.99C_{l_\beta} + 18.861$	$0.028C_{n_\beta} - 1.656C_{l_\beta} + 3.355$

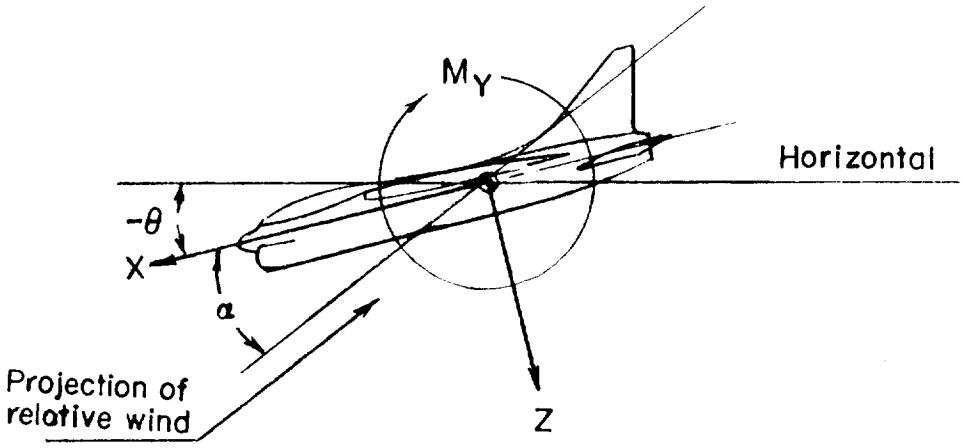

(a) ϕ and $\psi = 0$.

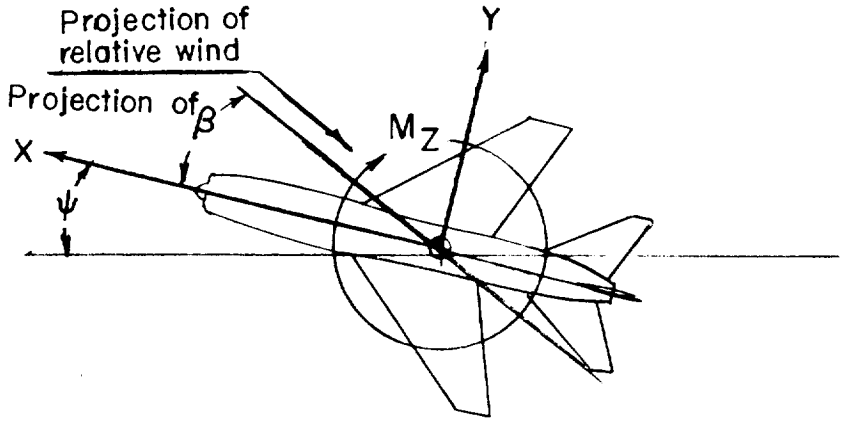

(b) θ and $\phi = 0$.

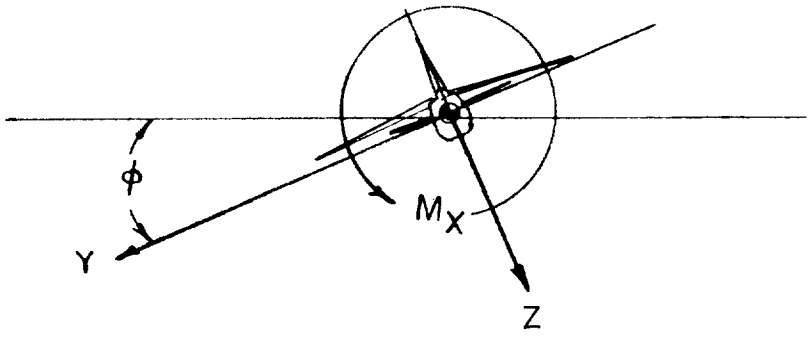

(c) θ and $\psi = 0$.

Figure 1.- Body system of axes and related angles.

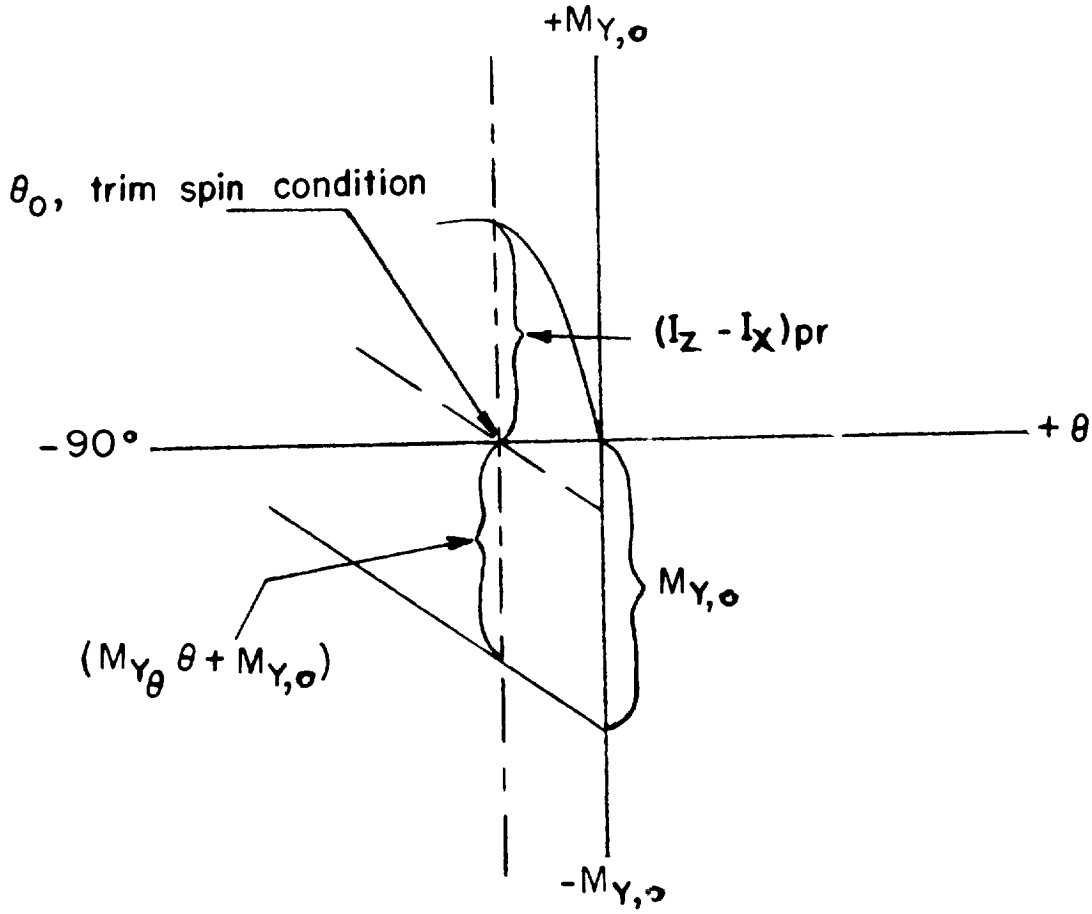

Figure 2.- Sketch indicating relative nature of various terms in pitching-moment equation.

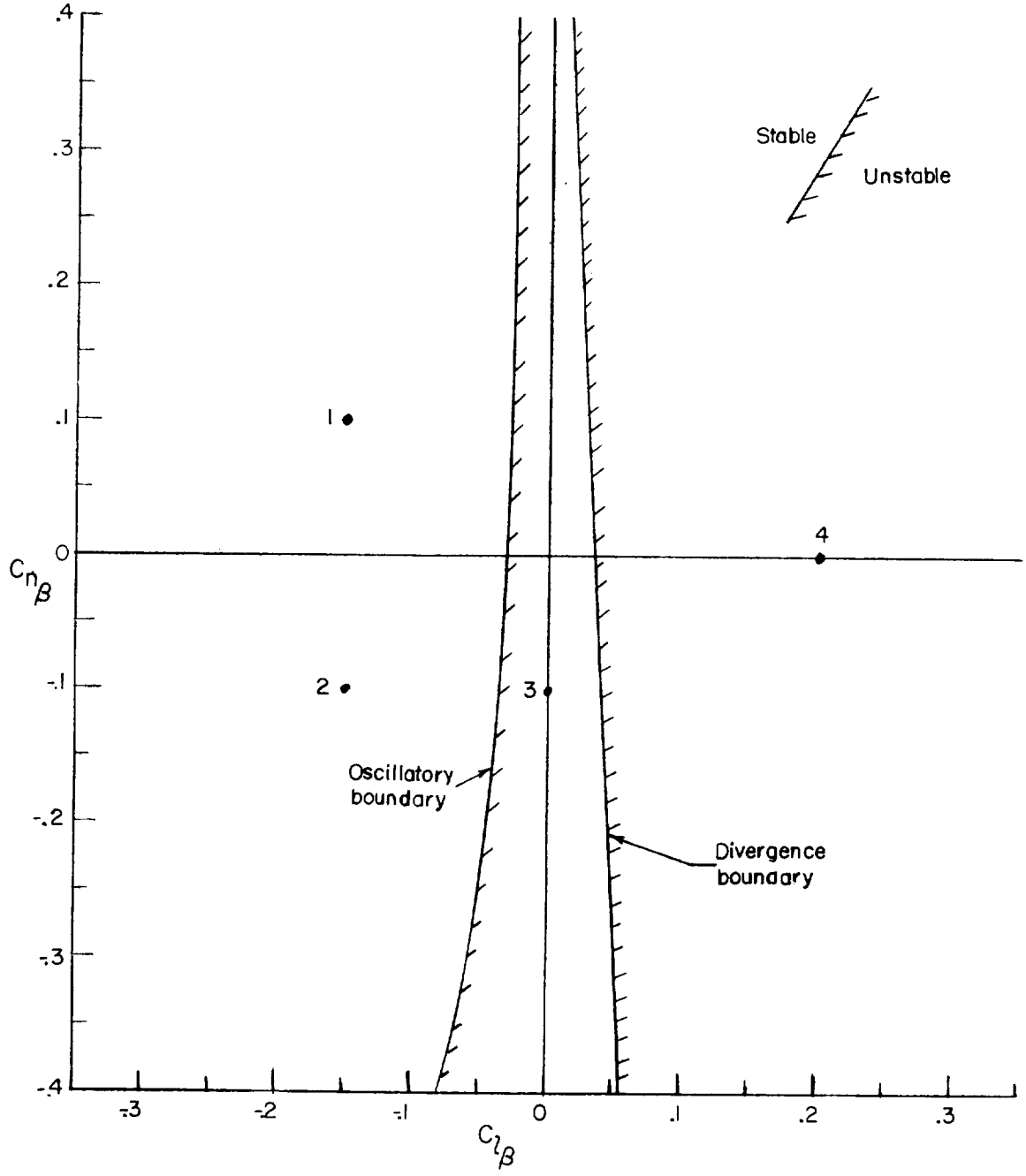

Figure 3.- Stability diagram for case A.

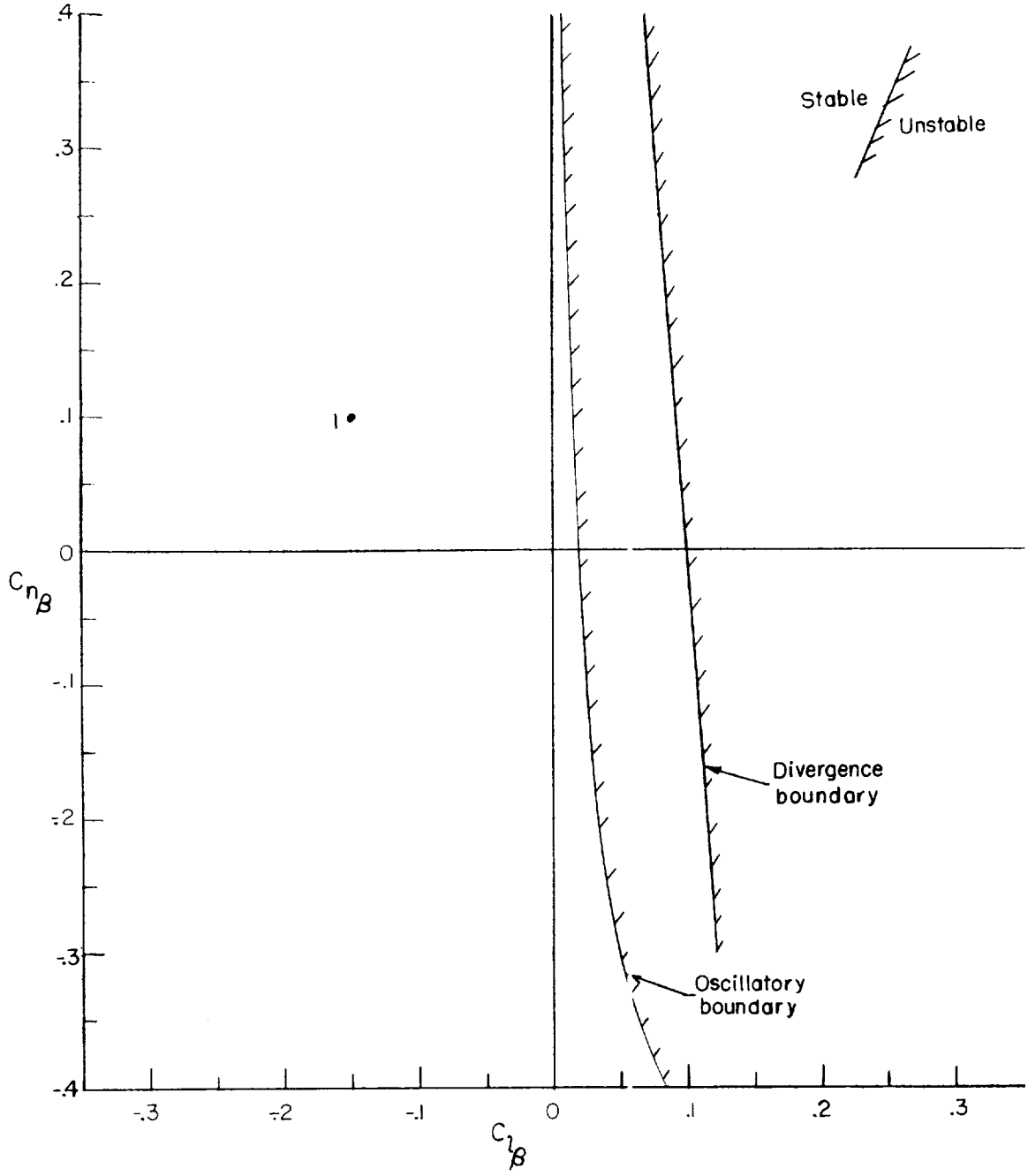

Figure 4.- Stability diagram for case B.

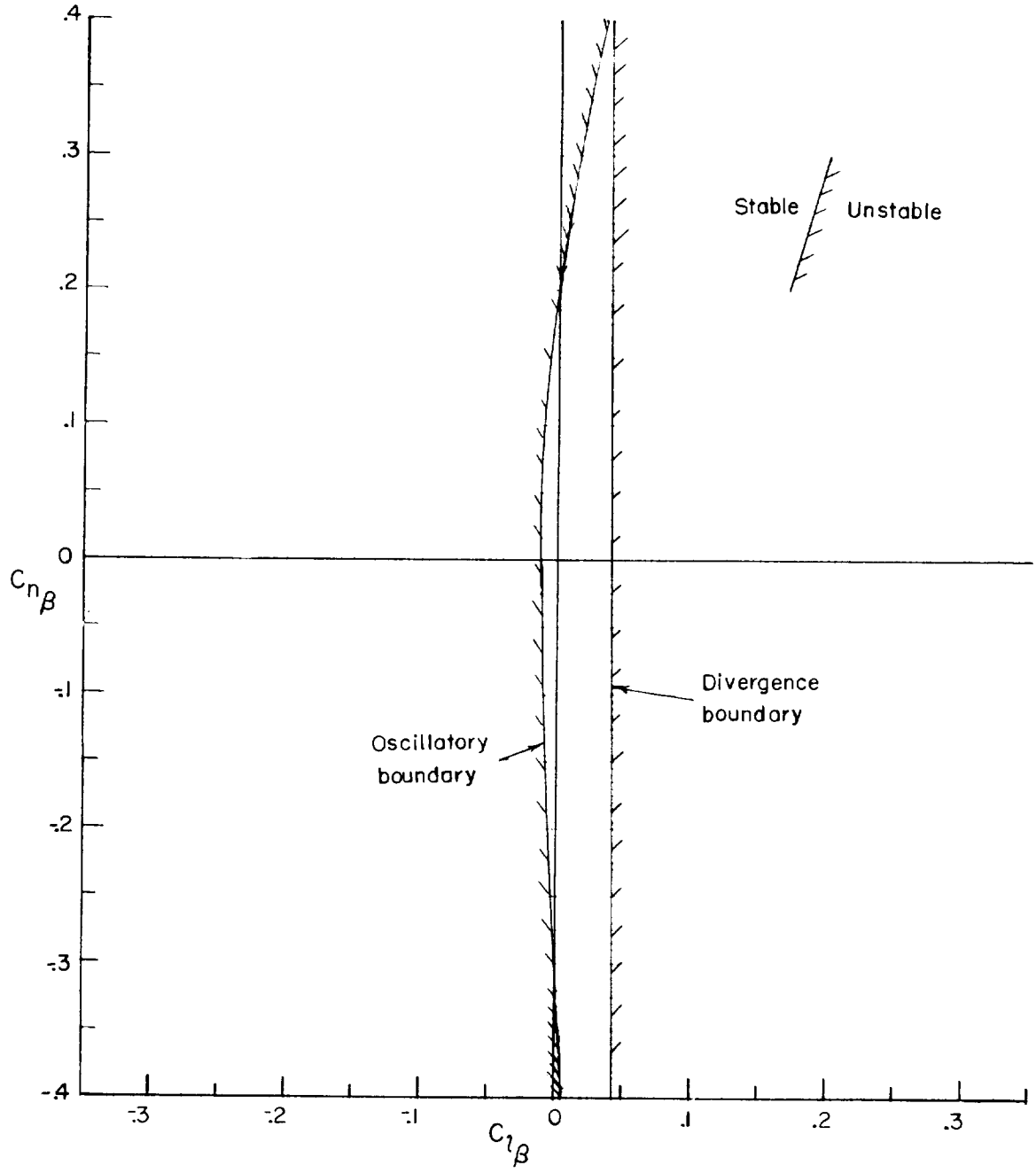

Figure 5.- Stability diagram for case C.

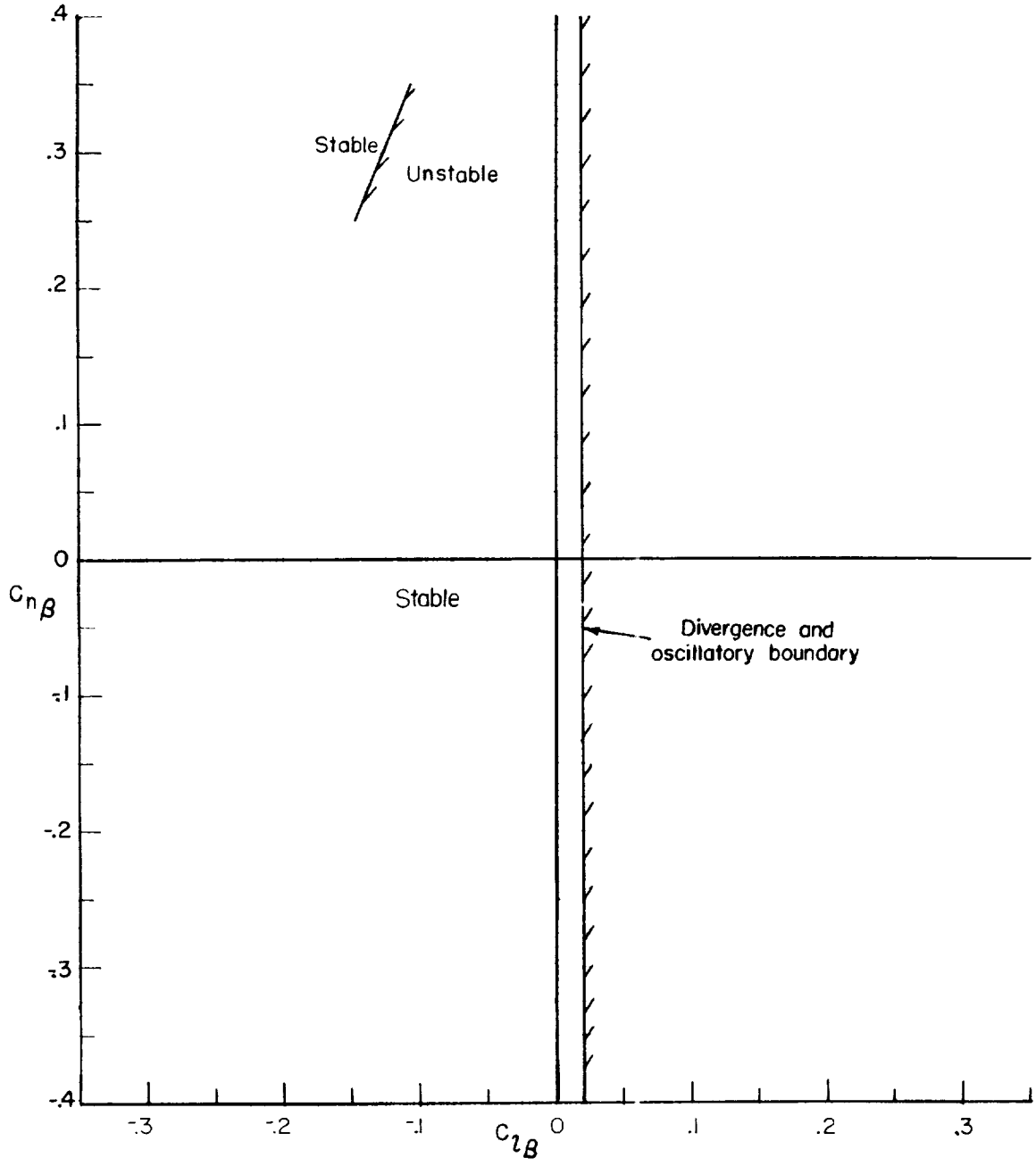

Figure 6.- Stability diagram for case D.

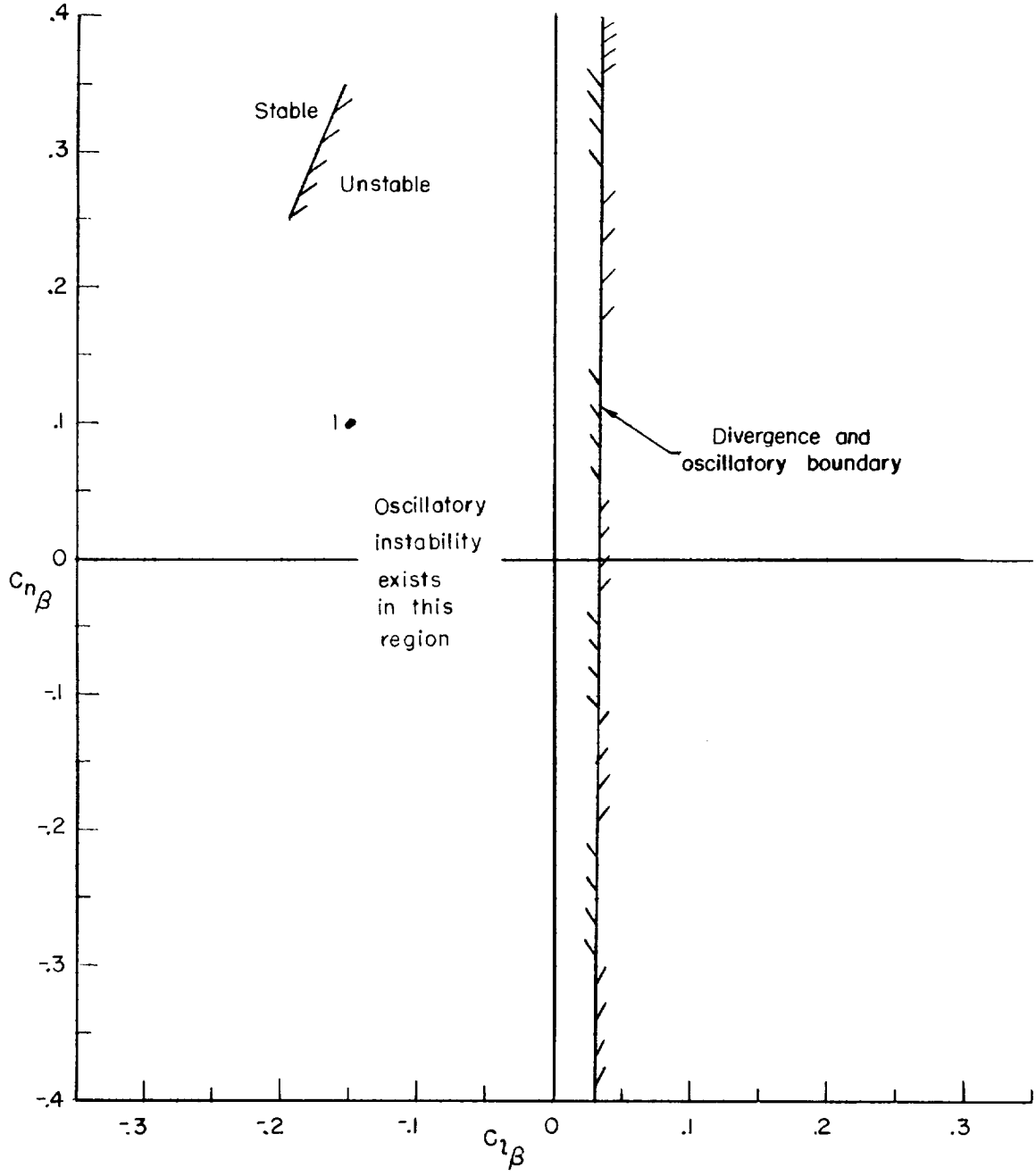

Figure 7.- Stability diagram for case E.

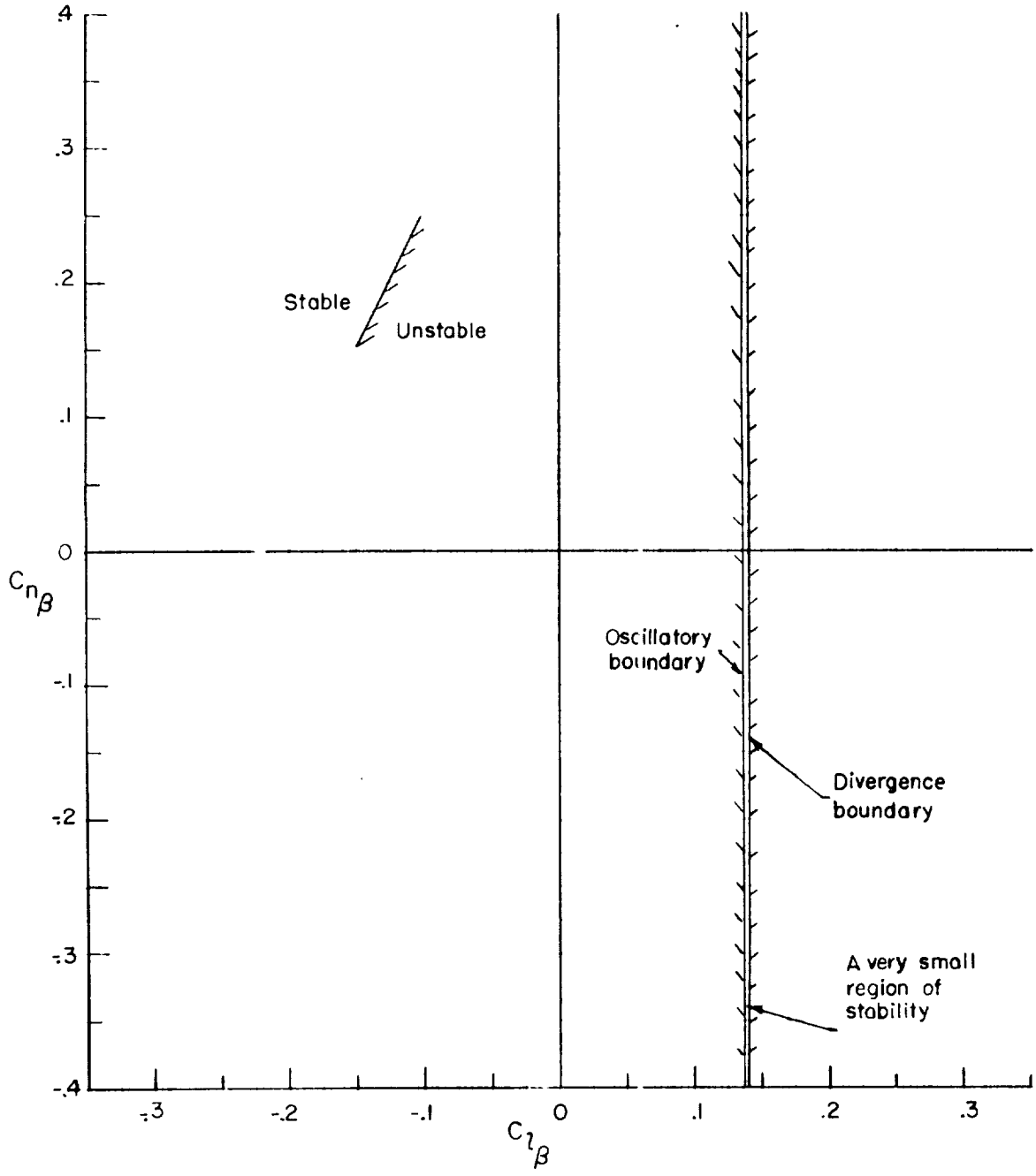

Figure 8.- Stability diagram for case F.

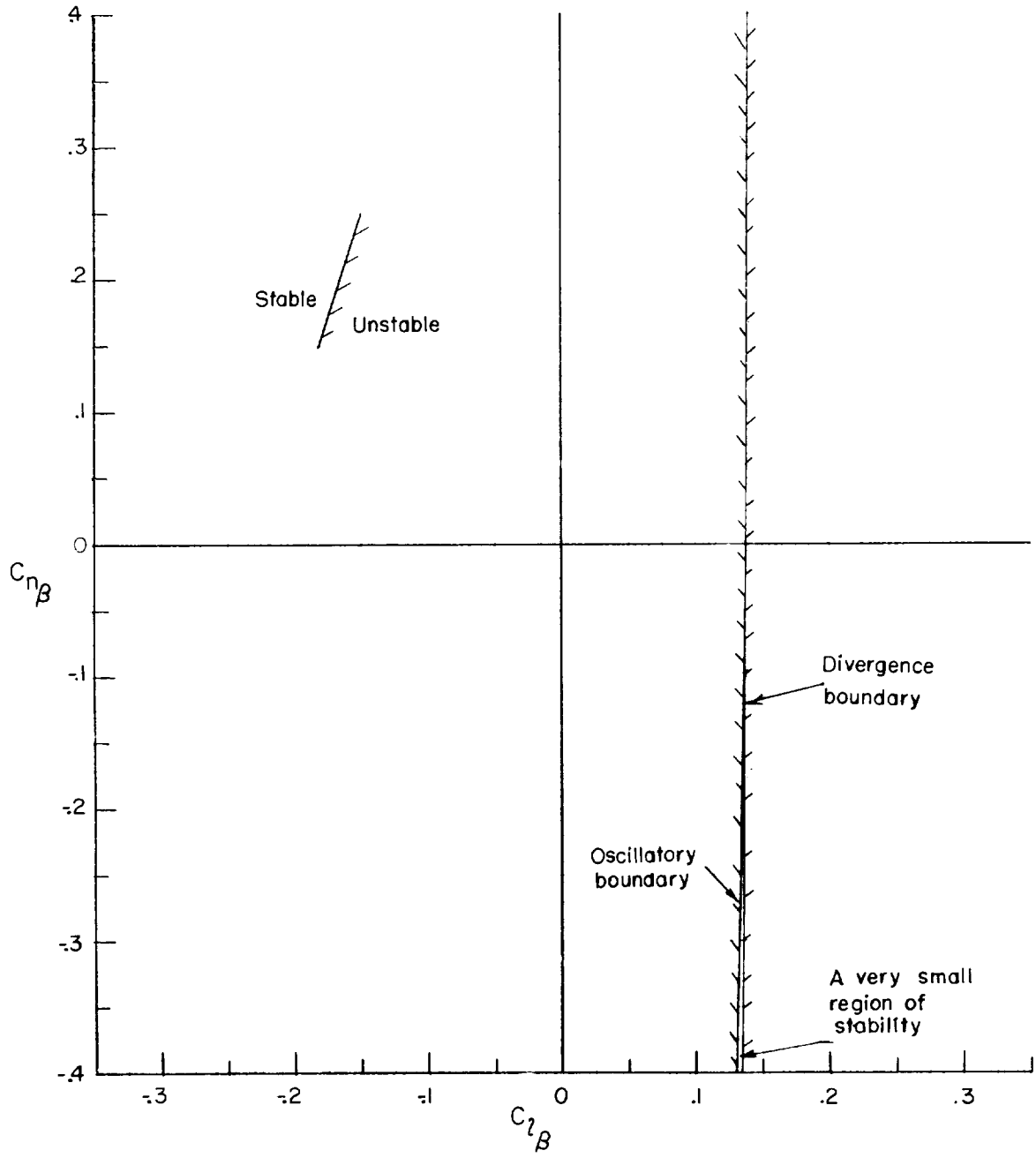

Figure 9.- Stability diagram for case G.

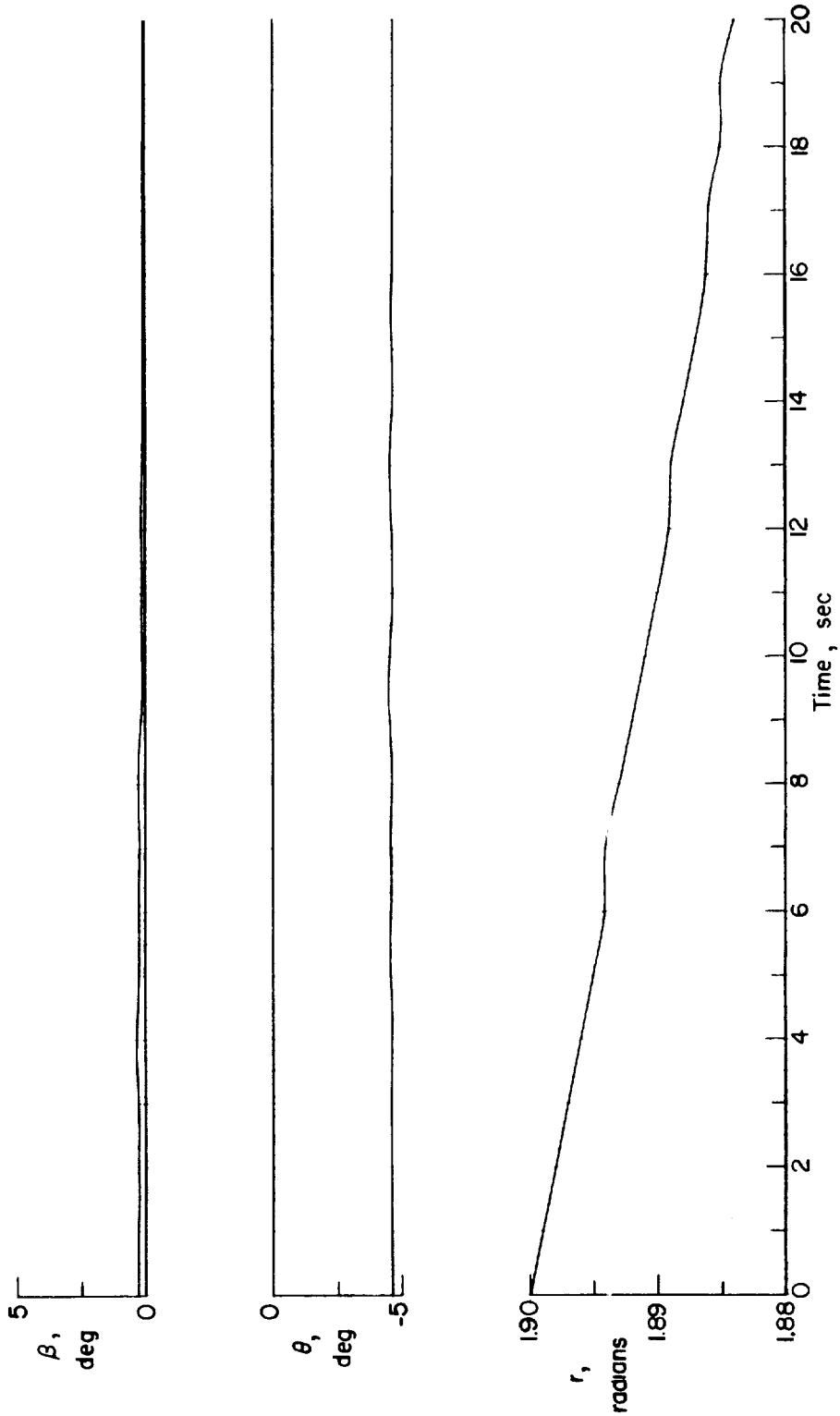

Figure 10.- Motion for point 1 of case A (fig. 3) with C_{l_p} acting (no rolling-moment coefficient applied).

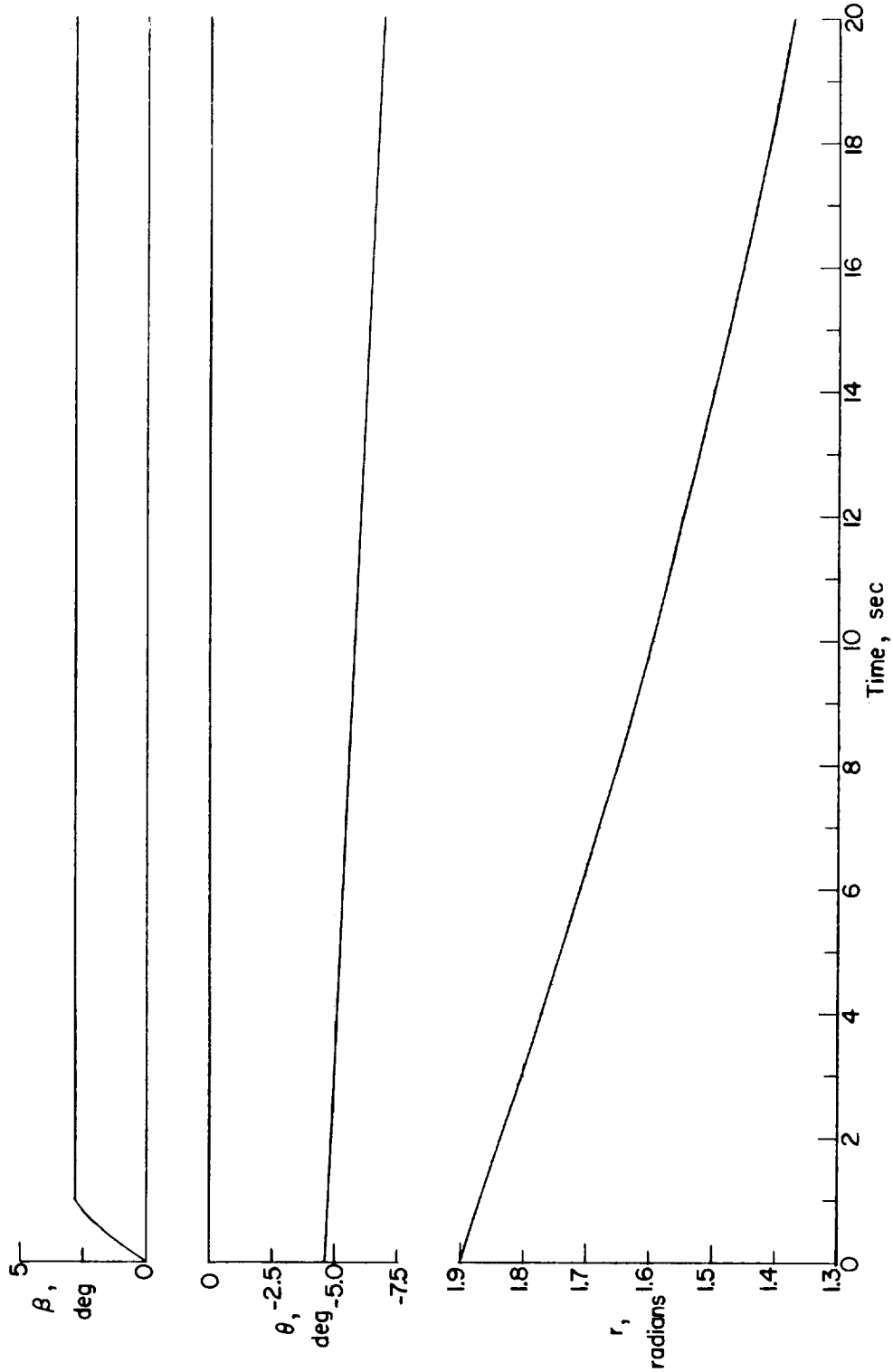

Figure 11.- Motion for point 2 of case A (fig. 3) after application of a rolling-moment coefficient of 0.01.

rolling-moment coefficient applied).

48

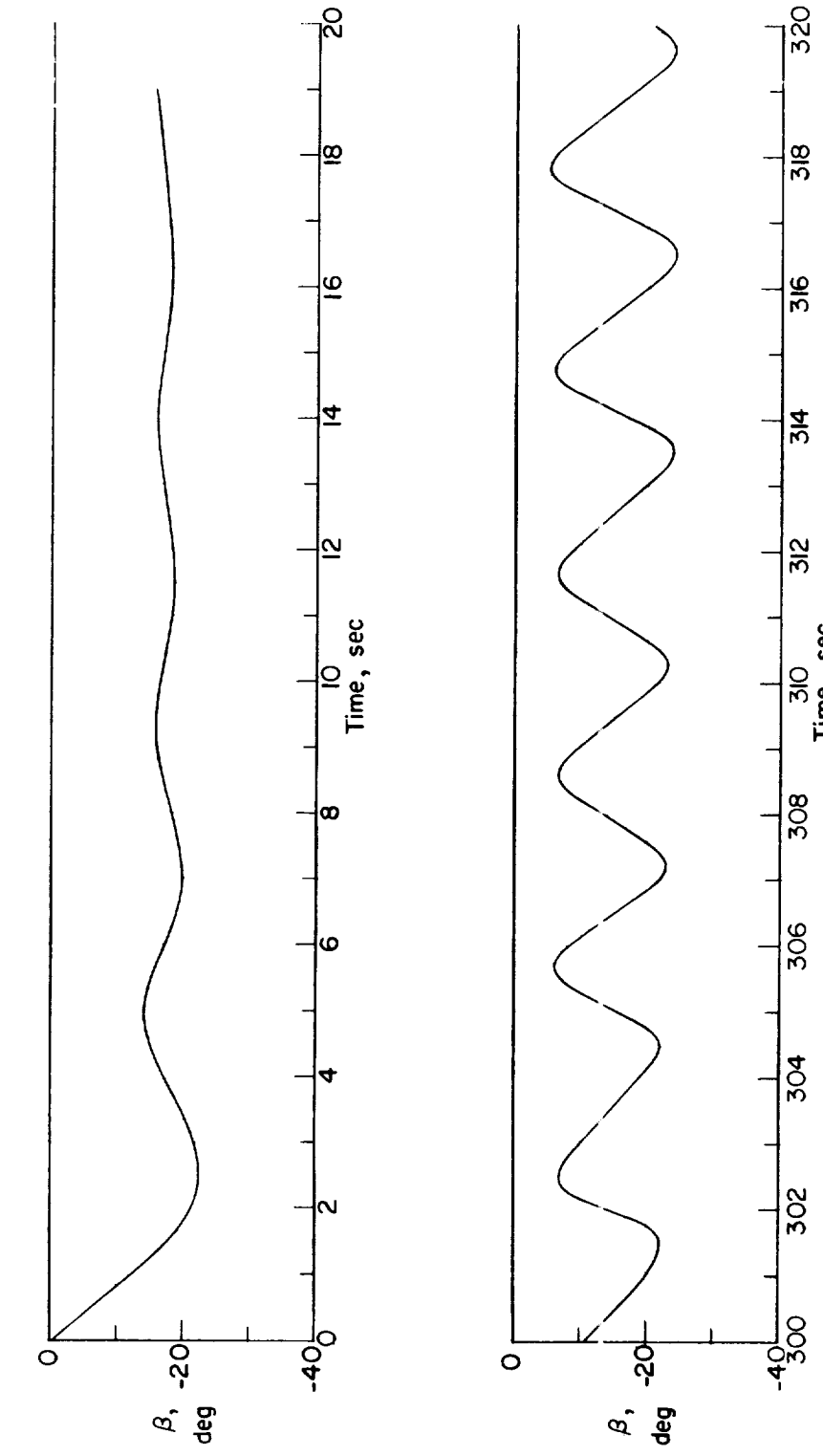

Figure 14.- Motion for point 3 of case A (fig. 3) after application of a rolling-moment coefficient of -0.01. (Note the time scales.)

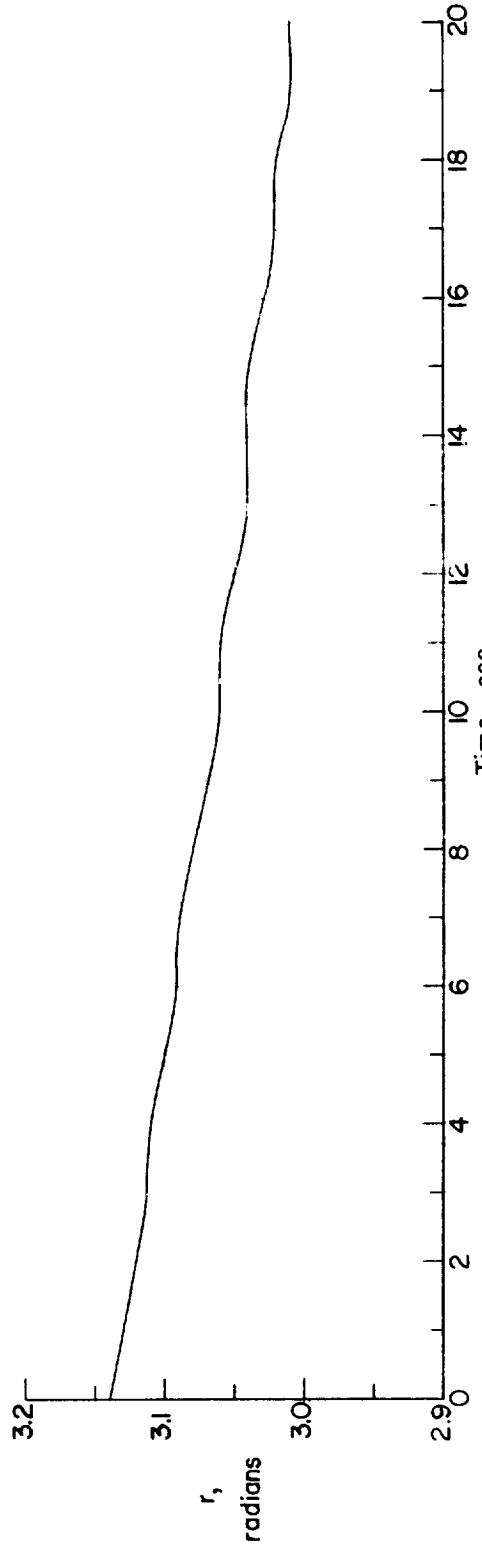

Figure 15.- Motion for point 1 of case B (fig. 4) after application of a rolling-moment coefficient of 0.01.

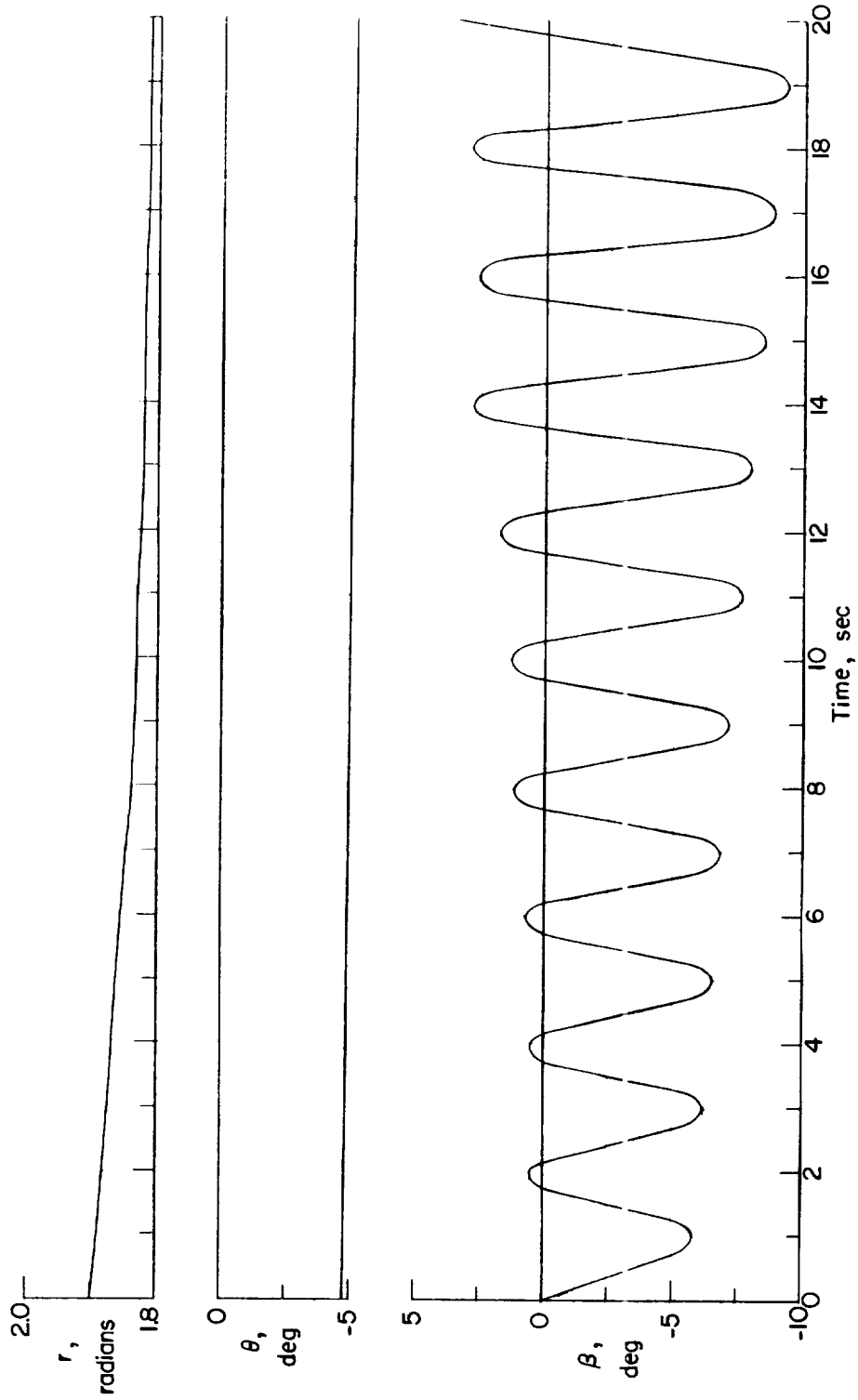

Figure 16.- Motion for point 1 of case E (fig. 7) after application of a rolling-moment coefficient of -0.01.